

**UNCLASSIFIED**

**AD 419216**

**DEFENSE DOCUMENTATION CENTER**

**FOR**

**SCIENTIFIC AND TECHNICAL INFORMATION**

**CAMERON STATION, ALEXANDRIA, VIRGINIA**

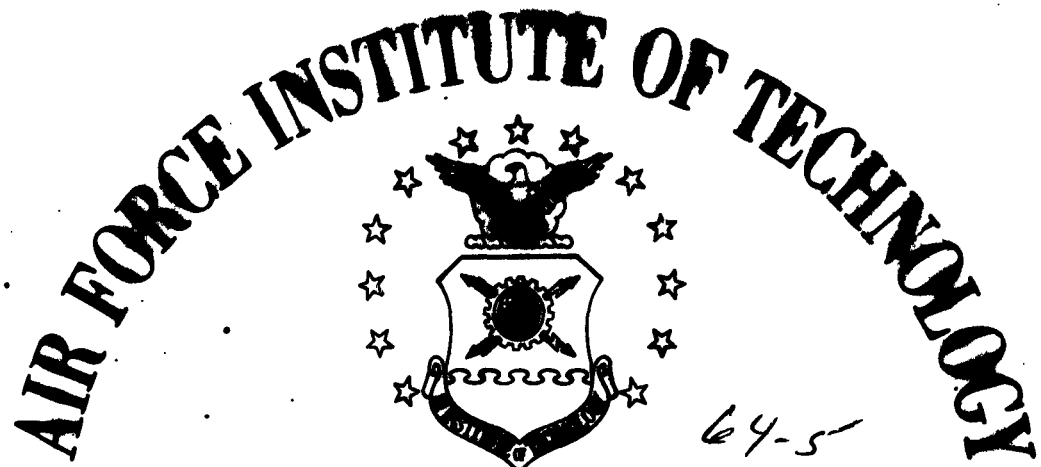


**UNCLASSIFIED**

NOTICE: When government or other drawings, specifications or other data are used for any purpose other than in connection with a definitely related government procurement operation, the U. S. Government thereby incurs no responsibility, nor any obligation whatsoever; and the fact that the Government may have formulated, furnished, or in any way supplied the said drawings, specifications, or other data is not to be regarded by implication or otherwise as in any manner licensing the holder or any other person or corporation, or conveying any rights or permission to manufacture, use or sell any patented invention that may in any way be related thereto.

419216

CATALOGED BY DDC  
AS AD. No. 419216

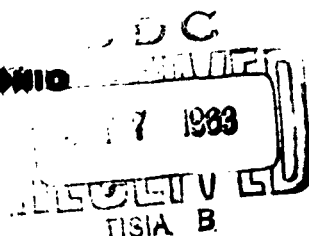


AIR UNIVERSITY  
UNITED STATES AIR FORCE



SCHOOL OF ENGINEERING

WRIGHT-PATTERSON AIR FORCE BASE, OHIO



MAGNETIC PROPERTIES OF A SERIES  
OF  
NICKEL-COPPER-IRON ALLOYS

Capt George L. Rosenhauer

GAE/Phys/63-1

MAGNETIC PROPERTIES OF A SERIES  
OF  
NICKEL-COPPER-IRON ALLOYS

THESIS

Presented to the Faculty of the School of Engineering  
of the Air Force Institute of Technology  
Air University  
in Partial Fulfillment of the  
Requirements for the Degree of  
Master of Science

By  
George L. Rosenhauer, B.S.  
Capt USAF  
Graduate Aeronautical Engineering  
August 1963

Preface

The material presented in this thesis is the result of my efforts to investigate the magnetic characteristics of a series of Ni-Cu-Fe alloys. My previous experience in the fields of metallurgy and solid state physics was nil. My only qualification was simply an innate curiosity. As a result, trial and error were borne of necessity and the experienced reader will understand the learning process involved. The texts "Structure and Change" and "University Physics" (Ref 5 & 9) were used primarily as an introduction to magnetism. I also found that "Principles of Electrical Engineering" (Ref 2) was a useful aid in understanding the fundamentals of electromagnetism.

And now it is a real privilege to acknowledge the debt due Mr. John Olson and Mr. Robert Patton for their assistance in the design and preparation of test equipment. Their suggestions concerning my experimental technique were invaluable. My special thanks to Dr. L. S. Pedrotti and Dr. Karl Strnat for their learned guidance through my first attempt at a scientific investigation.

Contents

	Page
Preface . . . . .	ii
List of Figures . . . . .	v
Abstract . . . . .	vii
I. Introduction . . . . .	1
Background . . . . .	1
Purpose of the Study . . . . .	2
General Outline of the Study . . . . .	2
II. Theory . . . . .	3
Ferromagnetism . . . . .	3
Curie Temperature . . . . .	6
Initial Permeability . . . . .	6
Analysis of Temperature vs. Initial Permeability	8
III. Experimental Investigation of the Magnetic Properties of a Series of Ni-Cu-Fe Alloys . . . . .	11
Basis for Experimental Procedure . . . . .	11
Preparation of Alloys . . . . .	13
Measurement of Curie Temperature . . . . .	20
Measurement of Initial Permeability . . . . .	28
IV. Discussion of Results and Conclusions . . . . .	38
Analysis of Alloy Preparation . . . . .	38
Analysis of Curie Temperature Measurements . . . . .	42
Analysis of Initial Permeability Measurements . . . . .	47
Conclusions . . . . .	51
Bibliography . . . . .	53
Appendix A . . . . .	54
Appendix B . . . . .	55
Appendix C . . . . .	56

Contents

	Page
Appendix D . . . . .	57
Appendix E . . . . .	58
Appendix F . . . . .	60
Appendix G . . . . .	71
Vita . . . . .	74

List of Figures

Figure	Page
1 Electron shells in an atom of iron . . . . .	4
2 Typical hysteresis loop and magnetization curve	8
3 Theoretical plot of initial permeability vs. temperature . . . . .	9
4 Superpositioning of available information on Curie temperature and initial permeability for Ni-Cu-Fe . . . . .	12
5 Photograph of primary source material on Curie temperature and initial permeability after superpositioning . . . . .	54
6 Induction furnace complex used to prepare large Ni-Cu-Fe and Ni-Cu slugs . . . . .	55
7 Slug produced by melting in the induction furnace . . . . .	15
8 Levitation furnace used to prepare Ni-Cu-Fe rods from pressed cylinders . . . . .	56
9 Enlarged end-view of fractured Ni-Cu-Fe rod showing spherical formation of $Fe_2O_3$ . . . . .	57
10 Microscopic view of Copper powder showing presence of very small particles . . . . .	58
11 Microscopic view of Nickel powder showing uniformity of grain . . . . .	59
12 Typical Ni-Cu-Fe rod specimen produced by levitation melting. The rod has been machined and marked . . . . .	19
13 Specimen holder used to measure Curie temperature of Ni-Cu-Fe rods . . . . .	22
14 Solenoid and dewar complex used in measuring Curie temperatures . . . . .	24

List of Figures

Figure	Page
15 Schematic of apparatus used to measure Curie temperatures . . . . .	25
16-17 Influence of heating rate on Curie temperature . . . . .	26-27
18-27 Measurement of Curie temperature on Ni-Cu-Fe rod . . . . .	60-69
28 Measurement of Curie temperature on Ni-Cu-Fe toroid . . . . .	70
29 Experimental results of Curie temperature measurements on Ni-Cu-Fe alloys . . . . .	71-73
30 Basic schematic of apparatus used to measure initial permeability of Ni-Cu-Fe alloy . . . . .	30
31 Actual scale drawing of iron yoke on which initial permeability measurements are attempted . . . . .	30
32 The compound toroid used as the mathematical model for the iron yoke and the Ni-Cu-Fe rod . . . . .	32
33 Magnetization curve @ 20°C used to determine initial permeability region for Ni-Cu-Fe toroid . . . . .	36
34 Measurement of Curie temperature on Ni-Cu-Fe rod . . . . .	41
35 Enlarged view of area investigated of Ni-Cu-Fe ternary showing results of Curie temperature measurements. Temperatures are indicated for high purity alloys . . . . .	43
36 Plot of magnetic induction B vs. temperature for Ni-Cu-Fe toroid . . . . .	48

Abstract

Investigation of the magnetic properties of a series of Ni-Cu-Fe alloys was motivated by the need for telemetry of human body temperature. Ni-Cu-Fe alloys were prepared by levitation melting of compressed chips of the pure metals. Over one hundred alloys were prepared in this manner and measurement of the individual Curie temperatures provided additional information for the Ni-Cu-Fe ternary. The area of the Ni-Cu-Fe ternary investigated was within the limits, 47-53% Copper, 40-48% Nickel, and 4-8% Iron. The Curie temperatures measured within this area varied from  $-67.6^{\circ}\text{C}$  to  $+157.5^{\circ}\text{C}$ . Measurement of the initial permeability of the Ni-Cu-Fe alloys was limited but it was found that magnetic saturation of the Ni-Cu-Fe alloy occurred at unusually low values of magnetic field intensity. The feasibility of the Ni-Cu-Fe alloy as an active element for telemetry of human body temperature was established.

MAGNETIC PROPERTIES OF A SERIES  
OF  
NICKEL-COPPER-IRON ALLOYS

I. Introduction

Background

With the advent of manned space vehicles, determining human physiological performance became a necessity. Measuring man's physical performance in space was one of the objectives of the recent "Project Mercury". A necessary step in attaining this objective was the measurement of human body temperature by telemetry. Early sensors used in the telemetry of human body temperature were "Thermistors", usually single crystals with a high resistance dependence on temperature. The early Thermistor proved to be inadequate due to the high sensitivity required for telemetry and the inherently low power available from the spacecraft.

To fill this inadequacy and meet the requirements of high sensitivity and low power consumption, the Thermophysics Branch, Materials Central, Wright-Patterson Air Force Base, Ohio, proposed the development of a magnetic sensor for use in the telemetry of human body temperatures. To optimize the sensitivity of such a device, the active element was to be made of a ternary Ni-Cu-Fe alloy. The choice of this alloy was made on the basis of earlier work done with Ni-Cu by the Thermophysics Branch. While this investigation was in progress,

GAE/Phys/63-1

further development of the Thermistor and its associated equipment solved the problem of high sensitivity and low power; however the Thermophysics Branch saw fit to continue this investigation.

Purpose of the Study

The general purpose of this study is to investigate the magnetic properties of a series of Ni-Cu-Fe alloys and their temperature dependence characteristics. In particular the properties of initial permeability and Curie temperature are to be investigated. As a specific goal, it is to be determined whether these alloys will permit practical measurement of human body temperatures and be compatible with telemetry requirements.

General Outline of the Study

The general plan of this study is to briefly review the basic theory involved with ferromagnetics, the specific definition of Curie temperature and initial permeability, and the application of this theory to the requirements of a human body temperature sensor. Emphasis is placed on the experimental investigation of the Curie temperatures and initial permeabilities of a series of Ni-Cu-Fe alloys. Finally, a discussion of experimental results and conclusions is presented.

## II. Theory

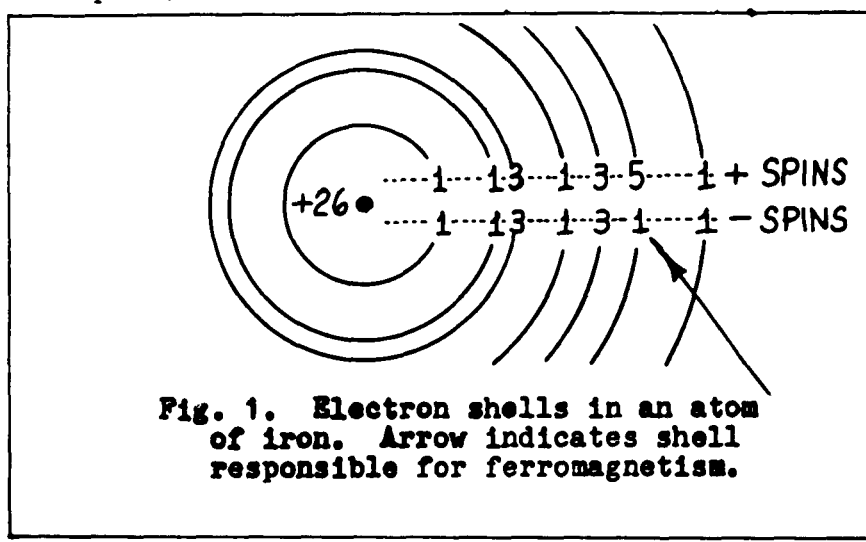
The purpose of this chapter is to present the fundamentals of ferromagnetism, define the ferromagnetic characteristics of Curie temperature and initial permeability, and show how these characteristics combine to fulfill the requirements of high sensitivity and low power. This chapter forms the theoretical platform for the investigation of the magnetic properties of the Ni-Cu-Fe series.

### Ferromagnetism

All substances can be divided into three general groups: ferromagnetic, paramagnetic, and diamagnetic. The reason for this division is that, within certain limitations, the magnetic qualities of each are markedly different. A ferromagnetic material has the familiar magnetic qualities of iron, while the paramagnetic and diamagnetic materials are almost non-magnetic in the presence of a field. For the purpose of illustration, consider small pieces of iron, manganese, and gold suspended on strings in an inhomogeneous field. The iron will tend to move toward the area where the field is strongest, the manganese will be weakly attracted toward the strong field, while the gold will tend to move toward the area where the field is weakest. This simple experiment demonstrates that the iron is ferromagnetic, the manganese paramagnetic, and the gold diamagnetic. However, at a unique temperature of 770 °C, the iron becomes paramagnetic. This phenomenon is

of particular interest in this study and will be discussed later.

To understand what happens to the iron in the presence of a magnetic field, the contribution of the fundamental magnetic particles, the spinning electrons, must be examined. The electrons which are responsible for the magnetic qualities of not only iron, but cobalt, nickel, and their alloys may be pictured as lying in a definite "shell" around the nucleus of the atom. In general, the total spin of the electrons in each shell is balanced. This means that for each electron spinning in one sense, there is another electron spinning in the opposite sense. In the case of the ferromagnetic material this balancing effect is not true, as shown in Fig. 1. The four unbalanced electron spins cause a magnetic polarization of the atom (Ref 3:435), and it behaves much like a small permanent bar magnet with a north and south pole.



An internal force called "exchange interaction" causes neighboring atoms, viewed as small permanent bar magnets, to line up in a parallel sense (Ref 3:427). This may result in a net magnetic moment great enough to permit a realignment of the spins, or small permanent bar magnets, when subjected to an external field. This realignment gives rise to the force evident when a piece of iron is placed near a horseshoe magnet. This concept of exchange interaction will be important later in the definition of Curie temperature.

An ordinary piece of iron does not behave like a permanent magnet under no-field conditions, at ordinary temperatures, because the internal force of exchange interaction is only strong enough to influence a limited volume. This volume is usually of the order of  $10^{-8}$  or  $10^{-9}$  cubic centimeters and is given the name "domain" (Ref 3:529). In the unmagnetized state the domains are arranged randomly such that the resultant magnetization of the specimen as a whole is zero (Ref 3:477). On the other hand, when an ordinary piece of iron is placed in a magnetic field, a net alignment of the domains results giving rise to a net magnetic moment for the entire sample, and the iron behaves as if it were magnetic.

The ferromagnetic material, the concept of exchange interaction, and the existence of domains are fundamental

to an understanding of Curie temperature and initial permeability.

#### Curie Temperature

The Curie temperature is defined as that temperature above which a ferromagnetic material no longer displays ferromagnetic characteristics. Above the Curie temperature the material becomes paramagnetic; for pure iron this temperature is 770 °C. Above the Curie temperature the ferromagnetic properties vanish since the disordering action of thermal agitation becomes strong enough to overpower the force of exchange interaction, thereby preventing the formation of domains. The Curie temperature for a Ni-Cu-Fe alloy is a function only of composition. It will be shown that definite changes in magnetic properties, especially initial permeability, take place at or near the Curie temperature.

#### Initial Permeability

In order to define initial permeability, normal permeability must first be understood. Permeability is an expression for the influence of a medium upon the resulting magnitude of the magnetic flux. The permeability  $\mu$  can be defined as:

$$\mu = \frac{B}{H} \quad (1)$$

where  $B$  is the flux density or magnetic induction in

gauss and  $H$  is the magnetic field intensity in oersteds. The quantities  $B$  and  $H$  represent the absolute magnitudes of the vector quantities  $\vec{B}$  and  $\vec{H}$ . For the situations discussed in this thesis,  $\vec{B}$  is always parallel to  $\vec{H}$  and vector notation has been omitted. The magnetic flux  $\phi$ , in maxwells, is defined as:

$$\phi = \iint \vec{B} \cdot d\vec{S} \quad (2)$$

For the case where  $B$  is uniform over the area  $S$ , equation (2) may be reduced to  $\phi = BS$ .

Combining (1) and (2) one obtains,

$$\phi = \mu H S \quad (3)$$

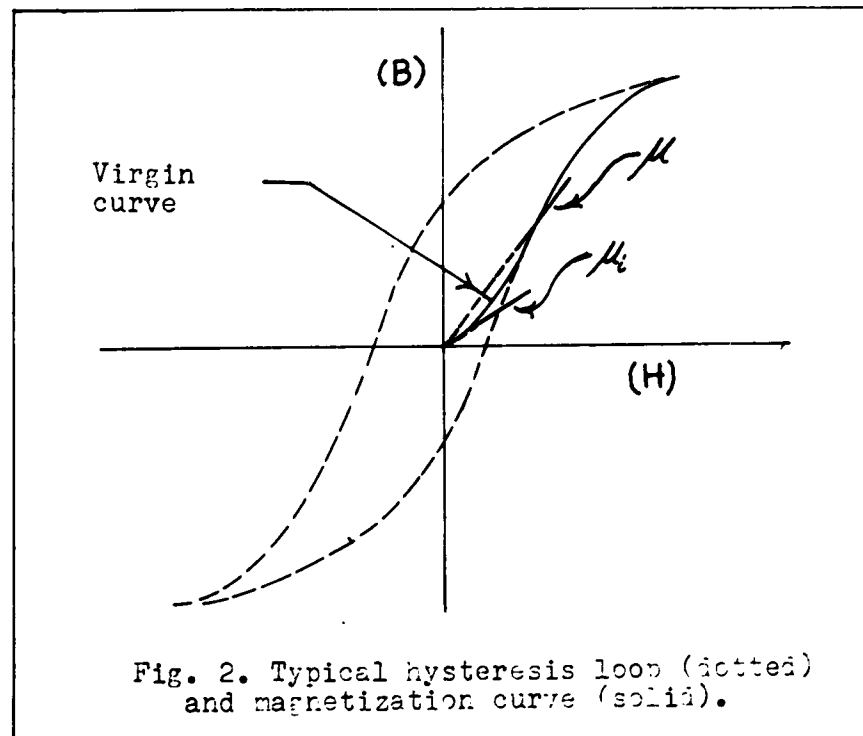
which is the relationship between the permeability and the resulting magnetic flux.

Based on equation (1), the initial permeability is defined as the limit of  $B/H$  as  $H$  approaches zero or,

$$\mu_i = \lim_{H \rightarrow 0} \frac{B}{H} \quad (4)$$

It follows from (4) that meaningful values of  $\mu_i$  must be obtained at extremely small values of field strength. Since the quantities  $\mu$  and  $\mu_i$  represent slopes of  $B$  vs.  $H$  curves, they can be shown on a plot of a typical hysteresis loop as in Fig. 2. The virgin curve in Fig. 2 means that the specimen was initially demagnetized.

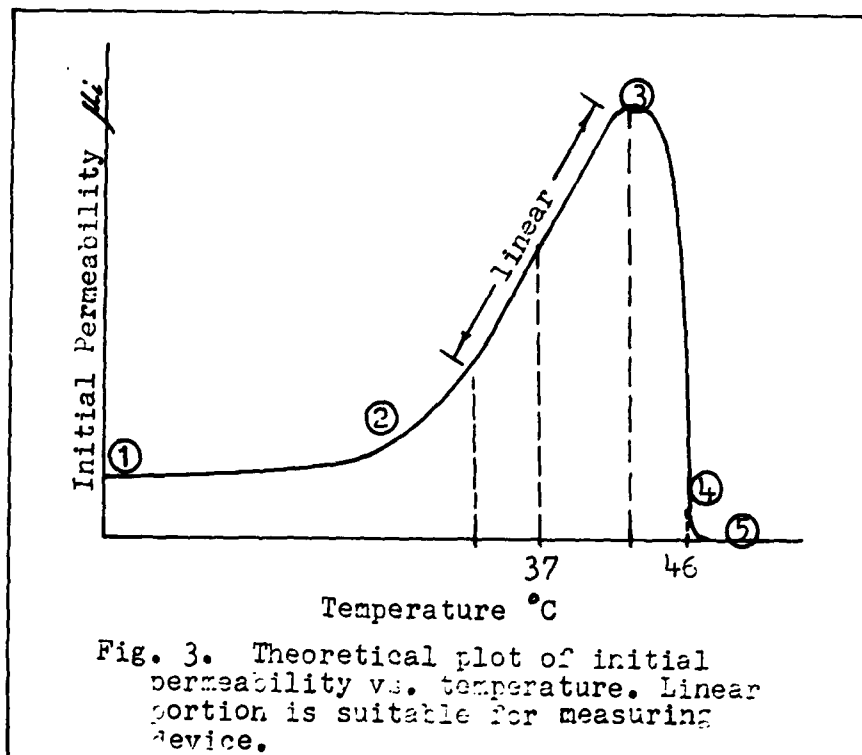
The initial permeability for a Ni-Cu-Fe alloy is dependent on heat treatment and can be as high as 12,000 gauss/oersted (Ref 1:99).



#### Analysis of Temperature vs. Initial Permeability

Curie temperature and initial permeability are both important considerations in the selection of an alloy for the active element of a sensing device of human body temperatures. A theoretical plot of initial permeability vs. temperature for a Ni-Cu-Fe alloy is given in Fig. 3. The

curve shown is for an alloy with a Curie temperature of  $46^{\circ}\text{C}$ . It is seen that the temperature dependence of the initial permeability is quite marked.



The portion of the curve from ① to ② shows very little change in  $\mu_i$  with temperature. At approximately  $32^{\circ}\text{C}$  the curve begins to rise linearly to very high values of  $\mu_i$ , as shown from ② to ③. It is this portion, from ② to ③, that could be utilized for sensing changes in human body temperature. Body temperature is normally  $37^{\circ}\text{C}$ , as shown, giving

GAE/Phys/63-1

an approximate range of  $7^{\circ}\text{C}$ , where  $35^{\circ}\text{C}$  and  $42^{\circ}\text{C}$  represent practical limits on human body temperature to maintain life. The portion from (3) to (4) is even more linear but the temperature range is too limited. The Curie temperature of  $46^{\circ}\text{C}$  is found by extrapolating the steepest slope from (3) to (4). The portion from (4) to (5) indicates the region where the ferromagnetic is changing to paramagnetic as mentioned earlier.

From theoretical considerations, it has been shown that a Ni-Cu-Fe alloy with a high initial permeability and a Curie temperature of approximately  $46^{\circ}\text{C}$  could display temperature dependence characteristics making it a feasible sensing element. The critical requirement of high sensitivity is met by a change in the measurable quantity  $\mu_i$  of the order of  $10^4$  gauss/oersted with a corresponding change in temperature of  $10^{\circ}\text{C}$  near the Curie temperature. The additional requirement of low power is met since  $\mu_i$  is defined only for very low fields  $H$ . The theory presented in this chapter motivates the experimental investigation of the magnetic properties of a series of Ni-Cu-Fe alloys.

### III. Experimental Investigation of the Magnetic Properties of a Series of Ni-Cu-Fe Alloys

The purpose of this chapter is to present the experimental procedure used in the course of this investigation. A departure point for the investigation, resulting from a literature search, is given first. Once a basis for experimental procedure is established, the preparation of alloys, the measurement of Curie temperature, and the investigation of initial permeability are presented. A description of apparatus is included with each progressive investigative step.

#### Basis for Experimental Procedure

From a search of available literature, two sources were selected as primary data on the Ni-Cu-Fe ternary. An investigation of Curie temperatures by Koster and Dannohl (Ref 6:223), and an investigation of initial permeabilities by Von Auwers and Neumann (Ref 1:98) were used. Superpositioning of these two investigations, as shown in the simplified ternary diagram of Fig. 4, provides graphic correlation of the material and definition of the area investigated. A photograph of the actual superpositioning, made by Mr. Patton of the Thermo-physics Branch, is shown in Fig. 5, Appendix A.

The salient features of Fig. 4 are the lines of constant initial permeability, the lines of constant Curie temperature, and the 625°C phase equilibrium line. The ternary diagram for

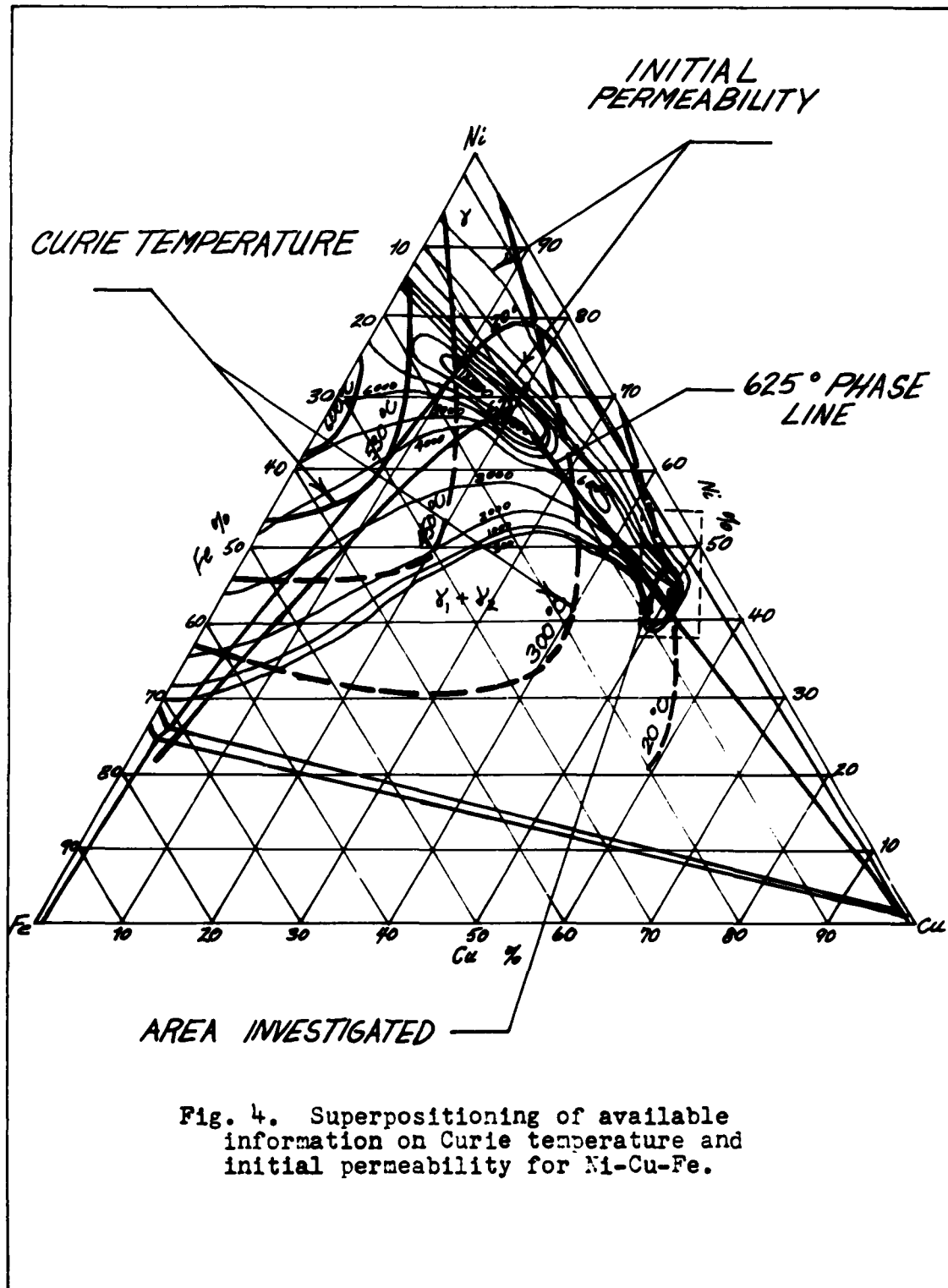


Fig. 4. Superpositioning of available information on Curie temperature and initial permeability for Ni-Cu-Fe.

Ni-Cu-Fe points out characteristics of interest about this alloy. The constant Curie temperature lines indicate a higher dependence on composition in the low temperature range. Near the 20°C line the temperature is markedly dependent on Fe content. Initial permeability is primarily a function of the history of the alloy and the lines shown on Fig. 4 were chosen because the method of heat treatment is a simple quenching process.

The area investigated is roughly defined by the dashed rectangle in Fig. 4. Within this area is included the 46°C Curie temperature line, areas of high initial permeability, and the presence of a single face-centered  $\gamma$  phase. The importance of the  $\gamma$  phase is discussed in a following section.

After defining the area of the Ni-Cu-Fe ternary to be investigated, the next step was to prepare the alloys.

#### Preparation of Alloys

Since the 20°C line in Fig. 4 is the only known data within the area investigated, more information on composition dependence of Curie temperature is needed. Obtaining this information requires the systematic preparation of a number of alloys. Preparation technique is extremely important because the magnetic properties of this alloy are highly sensitive to impurities. Four methods of preparation were

tried with only one giving reliable results. A brief description of each method is given before presenting the details of the final method of preparation. These early attempts at making alloys provide insight into the problems that must be considered.

Initial attempts were made to melt powders of Ni-Cu-Fe (assumed purity 99.9%) in an induction furnace, ref. Fig. 6, Appendix B. Melts were cast into slugs 1.25 cm in diameter and 6.5 cm long, as shown in Fig. 7. The weight of these slugs is 50 gm. Chemical analysis of these alloys showed 5-20% loss by weight of Fe. Severe attack of the alumina crucible was prevalent, often resulting in crucible failure and subsequent loss of the melt. The cause of loss of iron was not apparent at this time, but Curie temperature measurements gave inconsistent results and an alternate method of preparation was sought.

The second attempt to prepare the proper alloys consisted of two steps. First a binary Ni-Cu slug was prepared by induction melting. This slug was cut into small cylinders weighing approximately 20 gm. A small hole drilled in one end of each cylinder was filled with the desired amount of Fe based on the assumed Ni-Cu content by weight. The small cylinder was melted in a levitation furnace as shown in Fig. 8, Appendix C. The levitation furnace eliminated the need for a crucible when melting with Fe present. After melting in

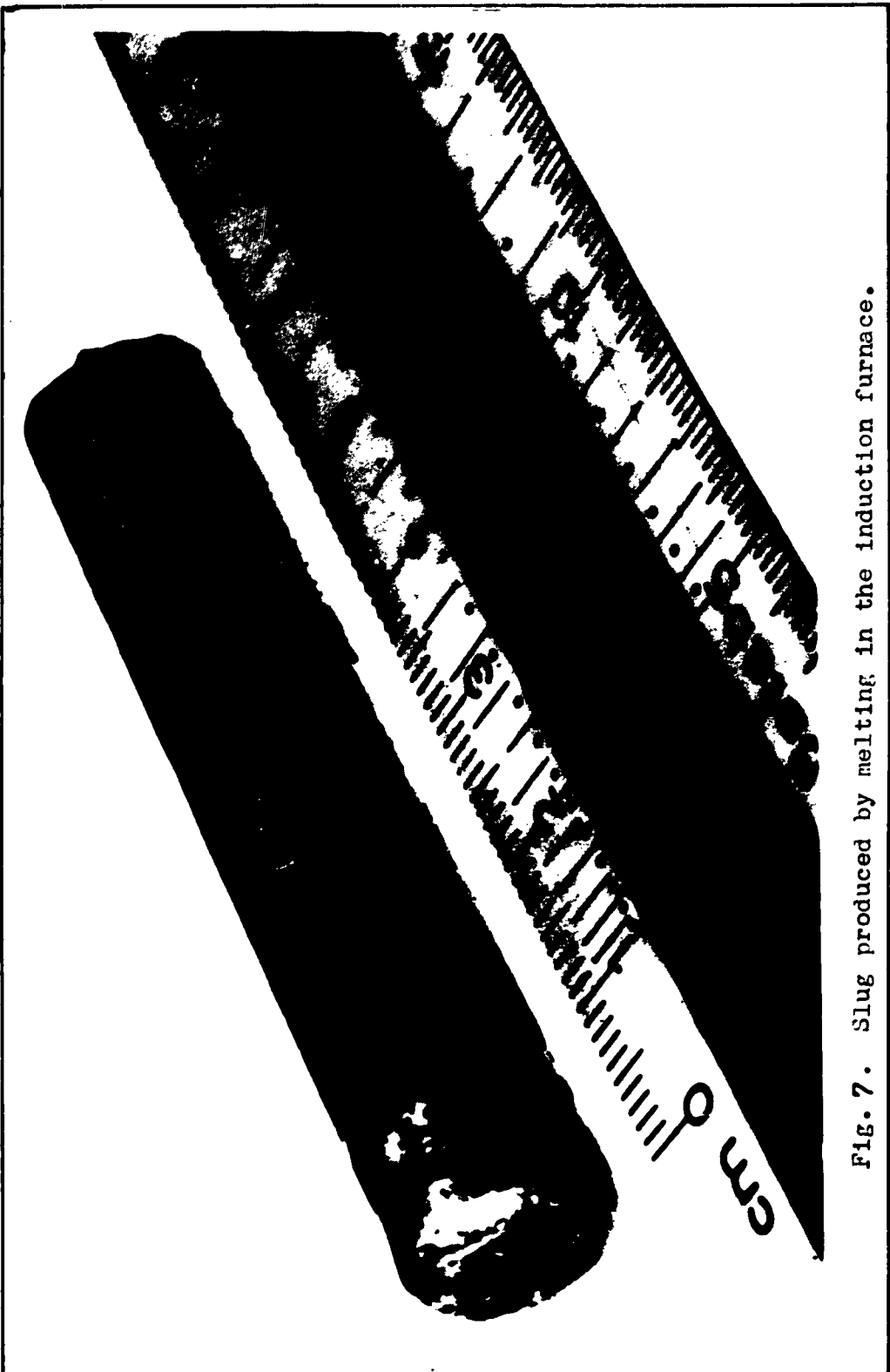


FIG. 7. Slug produced by melting in the induction furnace.

in the levitation furnace the alloys were cast into small rods 3.75 cm long and 0.625 cm in diameter. Curie temperature measurements of this series of melts agreed closely with the known 20°C Curie temperature line, but the involved procedure of double melting and adding Fe was impractical.

The next preparation attempt eliminated the induction furnace entirely. A 1.25 cm cylindrical die was made from steel, heat treated, and hardened. With a hand-operated hydraulic press, the cylindrical die was used to press the metal powders into small cylinders weighing 10 gm. A pressure of 50,000 psi gave densities close to 90%. The cylinders were melted in the levitation furnace and again cast into small rods. During casting, fracture of one of these rods yielded a great deal of information.

Examination of the broken rod showed the internal formation of an appreciable amount of  $Fe_2O_3$ , ref. Fig. 9, Appendix D. Since the induction furnace had been eliminated, the levitation furnace had been evacuated to 50 microns, and melting accomplished in a pure Argon atmosphere, the oxygen present had to come from the powders. Microscopic examination of the metal powders indicated a large number of very small particles in the Cu and Fe, while the Ni was uniform. A comparison of the Cu and Ni powders is shown in Figs. 10 and 11, Appendix E. The surface to volume ratio of the metals had to be decreased.

Several combinations of sizes and geometries were tried in the hydraulic press. Extremely good results were obtained by pressing chips made with a milling machine from large bars of pure Ni and Cu. The Fe chips were made from very pure platelets. This technique resulted in a reliable method of preparing pure alloys, the details of which are now given.

The initial procedure was to make a large chart of the area defined in Fig. 4. From the results of 60 alloys prepared by the previous methods a rough estimation of composition dependence of Curie temperature was made. Forty-five alloys covering the area of interest were prepared using chips. Alloys were selected by following lines of constant Fe content and allowing the Ni and Cu content to vary. In this manner, lines of constant Curie temperature were made parallel to the known 20°C line.

Chips of 99.9% pure metal were weighed to five significant figures with a total weight of 10 gm. The molds in the levitation furnace used to cast the small rods required 10 gm of material, and after pressing, 10 gm yielded a small cylinder with a length almost equal to its diameter. This geometry approximates a sphere and provides stability in the field of the levitation furnace.

After weighing, the chips were placed in the 1.25 cm cylindrical die and with a hand-operated hydraulic press were

compressed under 50,000 psi into small cylinders. These cylinders were again weighed to five significant figures, showing no appreciable loss during pressing.

The cylinders were placed in the levitation furnace, the chamber was evacuated to 50 microns, and melting accomplished at a third of an atmosphere in pure Argon. A third of an atmosphere provided further outgassing during melting. The field of the levitation furnace was slowly reduced, funneling the molten alloy into a copper mold just below the levitation coils. A rod 1.5 inches long and 0.5 inches in diameter was cast. The rods were weighed again, showing a loss after melting of approximately 0.25 of 1% or less. After machining to facilitate handling and measurement of magnetic properties, the rods appear as in Fig. 12.

The final step in the preparation of the Ni-Cu-Fe alloys was the heat treatment or annealing. The rods were placed in ceramic boats and heated to 1150°C in an annealing furnace. The furnace was first evacuated and then kept at a constant overpressure using pure Argon. The rod specimens were homogenized at 1150°C for 24 hours, cooled to 625°C, and quenched in water. The 24 hour period insured homogeneity of the specimen and quenching at 625°C insured presence of the single  $\gamma$  phase. Quenching from a temperature below the equilibrium line was likely to precipitate the  $\gamma+\gamma_2$  phase. The presence of two phases was undesirable because

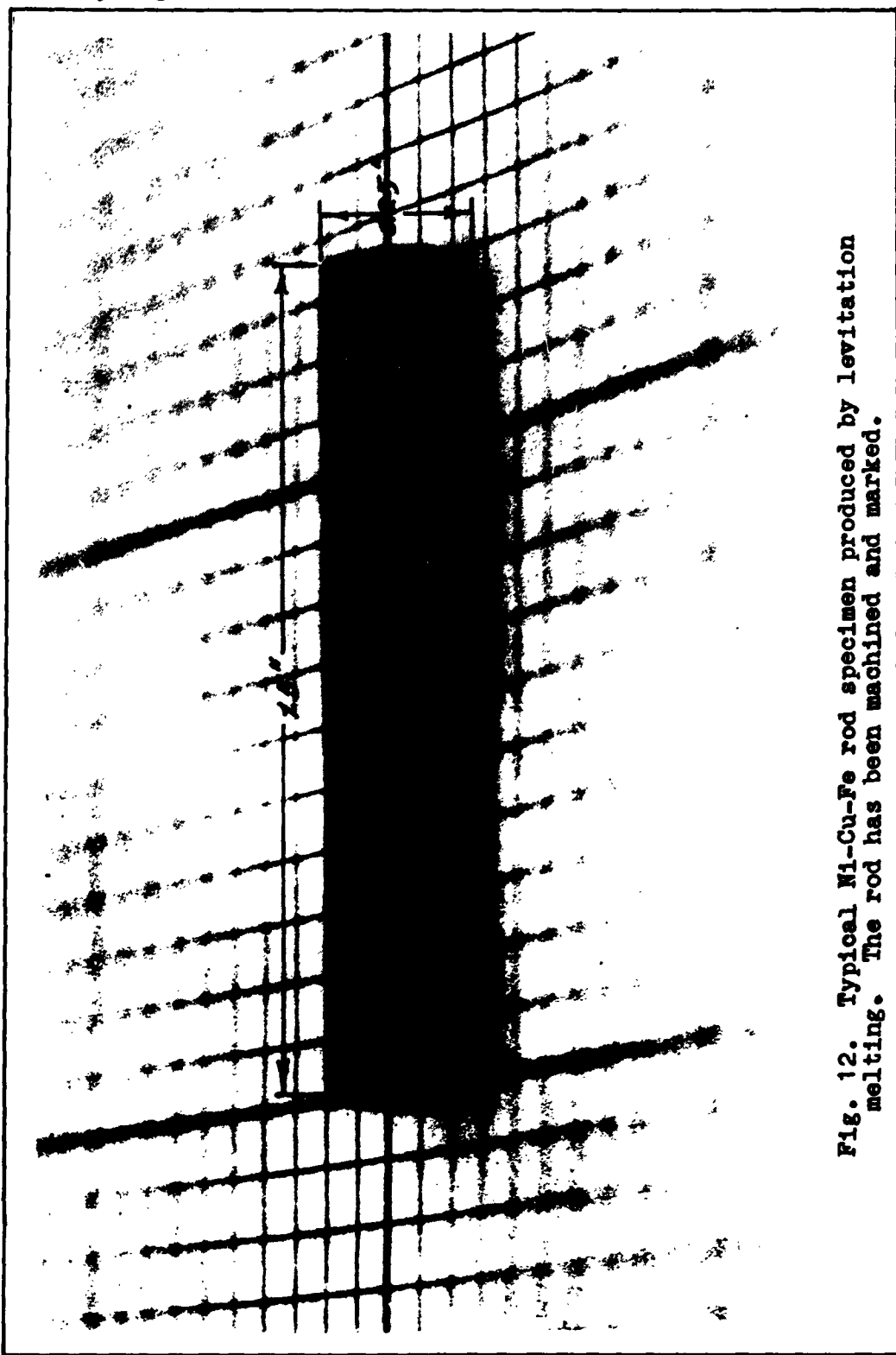


Fig. 12. Typical Ni-Cu-Fe rod specimen produced by levitation melting. The rod has been machined and marked.

one phase is copper-rich and has a different Curie temperature. As a result, the linear portions of the initial permeability vs. temperature curve shown in Fig. 3, Chapter II. become irregular and would not be suitable for a temperature measuring device.

Measurement of Curie Temperature

The second major objective of this study was to measure the individual Curie temperature of each rod. The purpose of this section is to present the theoretical considerations and experimental procedure used to measure the Curie temperatures of the Ni-Cu-Fe alloys.

Theoretical considerations provided a basis for the design of apparatus to measure Curie temperature. As discussed in the theory of Chapter II, a ferromagnetic material near its Curie temperature behaves similarly to a paramagnetic material. The Curie temperatures of the Ni-Cu-Fe alloys were to be obtained by determining the change in behavior from ferromagnetic to paramagnetic. The change from ferromagnetic to paramagnetic behavior is accompanied by a reduction in the permeability of the ferromagnetic material. Consider a secondary coil of copper wire in the presence of a varying field set up by a changing current in a primary circuit. An emf is induced in the secondary coil or "pickup coil", the magnitude of which is dependent upon the mutual inductance and the rate of change of current in the primary.

Since the mutual inductance is directly dependent on the permeability of the core of the secondary coil, a change in this permeability will be reflected by a change in the induced emf. The Curie temperatures were determined by using the Ni-Cu-Fe rods as cores in a secondary coil and measuring the change in induced emf near the Curie temperature of the core.

A specimen holder was designed to permit measurement of Curie temperatures of the Ni-Cu-Fe rods, as shown in Fig. 13. A solid 3/4" rod of bonded wound linen was used because it had the desirable properties of being nonmagnetic, having a high temperature capability, and being machinable. A 0.625 cm hole was drilled in one end of the holder to accomodate the Ni-Cu-Fe rod. A smaller hole, to accomodate the ceramic tube containing the thermocouple leads, was drilled the remaining length of the holder. To hold the pickup coil winding a 1.25 cm slot was machined with a 0.020 inch wall thickness, giving a close fit between the pickup coil and the rod specimen. A tungsten spring and a teflon disc were located just above the specimen to provide positive contact between the Ni-Cu-Fe rod and the thermocouple bead. A bucking coil was placed further up the specimen holder and wound oppositely to the pickup coil thereby cancelling the emf induced in the pickup coil due to the air core alone. Any output of the pickup coil is thus entirely due to the influence of the

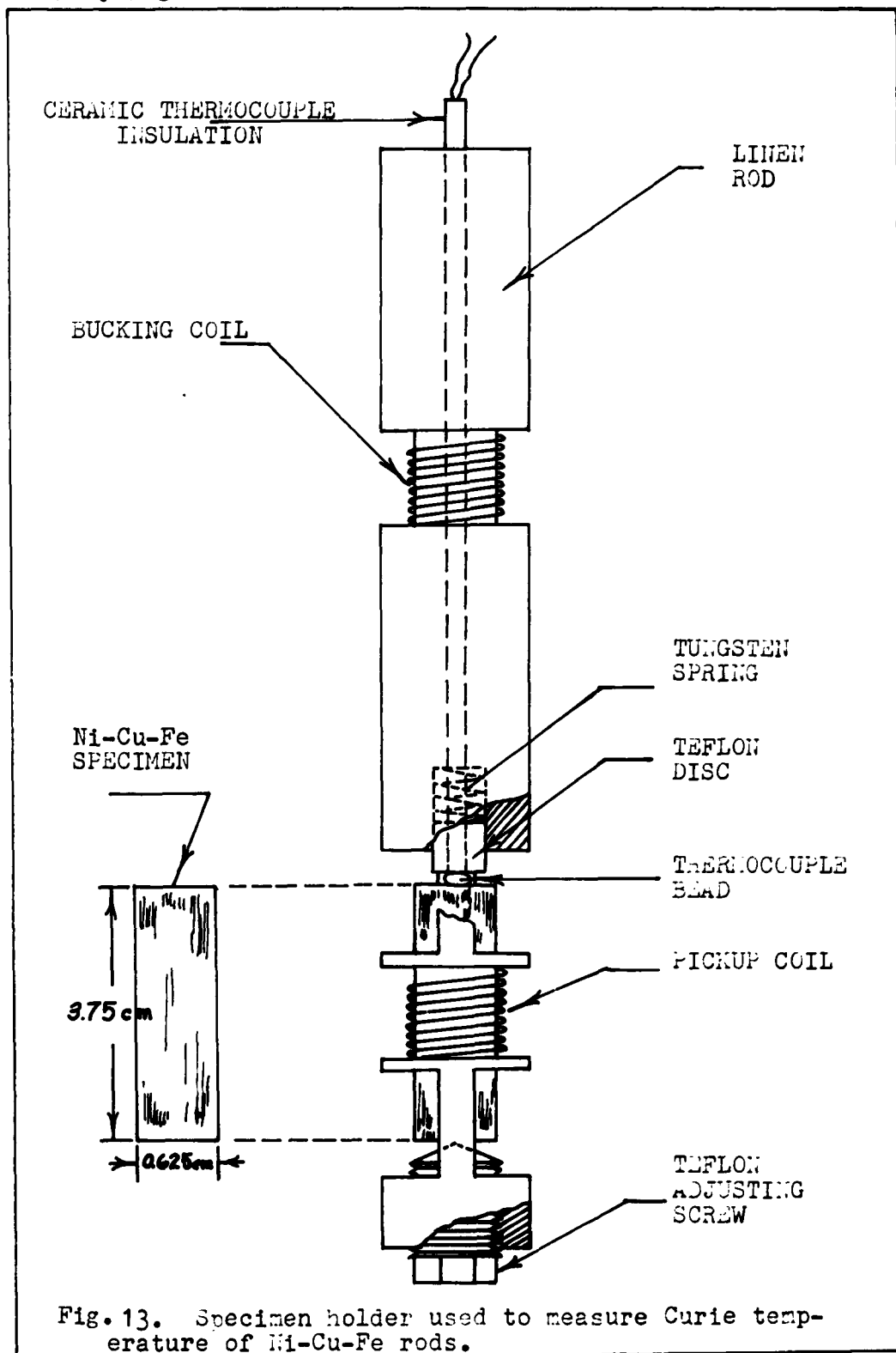


Fig. 13. Specimen holder used to measure Curie temperature of Ni-Cu-Fe rods.

Ni-Cu-Fe core. Below the specimen is a threaded teflon adjusting screw used to center the specimen in the pickup coil. Above and below the pickup coil are large windows for thermal contact between the specimen and the heating liquid.

The specimen and specimen holder were placed in the solenoid and dewar complex shown in Fig. 14. The liquid surrounding the specimen holder, depending on temperature range, was either water, glycerin, or methanol-LN<sub>2</sub> slush. The inner specimen chamber is designed to provide a uniform temperature gradient between the walls and the liquid surrounding the specimen holder. The outer liquid used was glycerin because of its high boiling point (290°C). A compact nichrome heater was designed and used with a DC power source to avoid interference with the pickup coil. This entire arrangement was contained in a glass dewar placed inside the field solenoid. Additional equipment is shown in the schematic of Fig. 15.

The current to the field solenoid was set at .05 amp and runs were made to roughly determine the Curie temperature of the specimen. The rough run permits better utilization of time during the actual run since a heating rate of 0.5 C° per minute near the Curie temperature is desired. A study to determine the influence of the heating rate on the extrapolated Curie temperature is shown by Fig. 16 and Fig. 17. A copper-constantan thermocouple and an ice-water reference

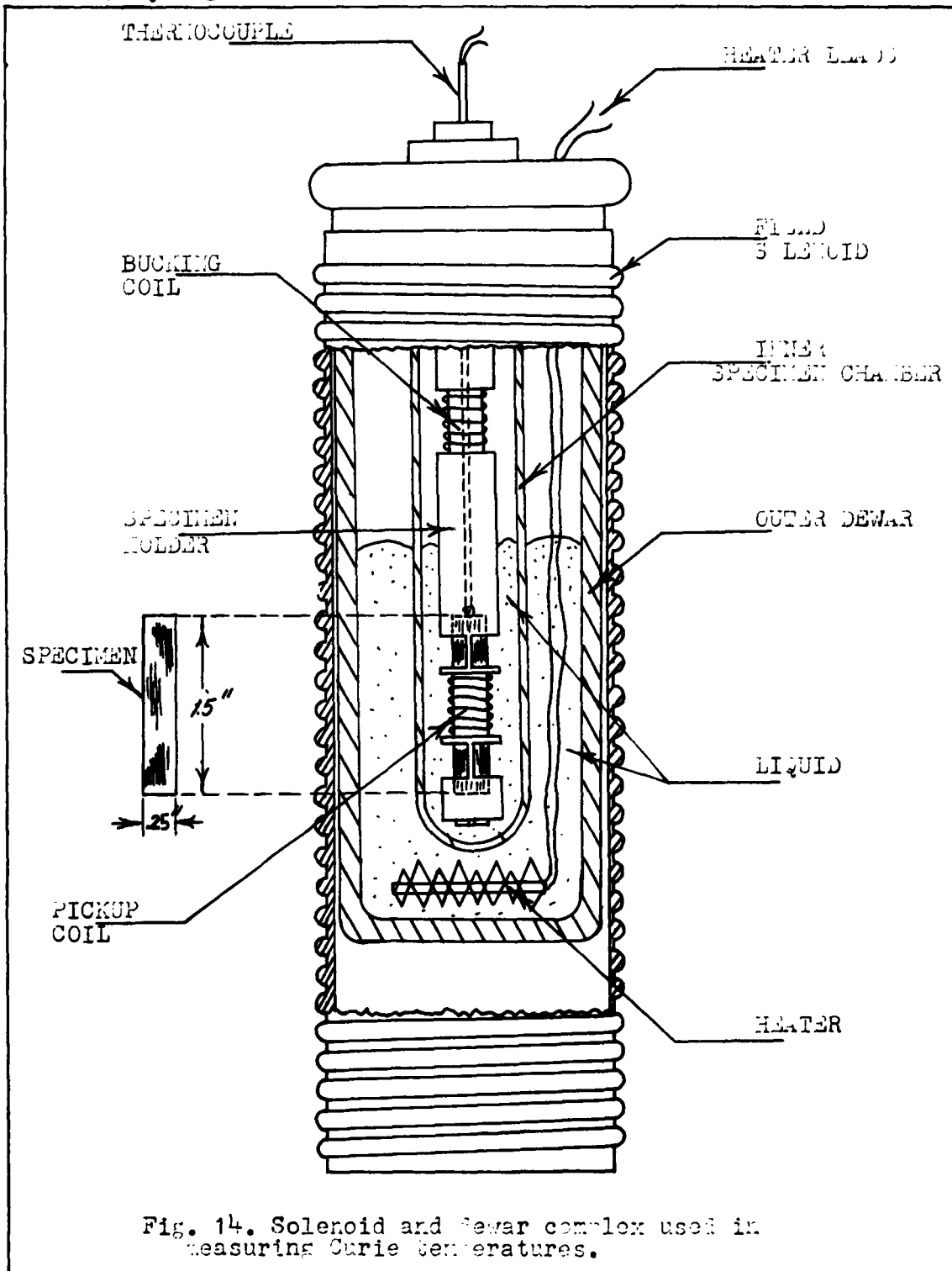
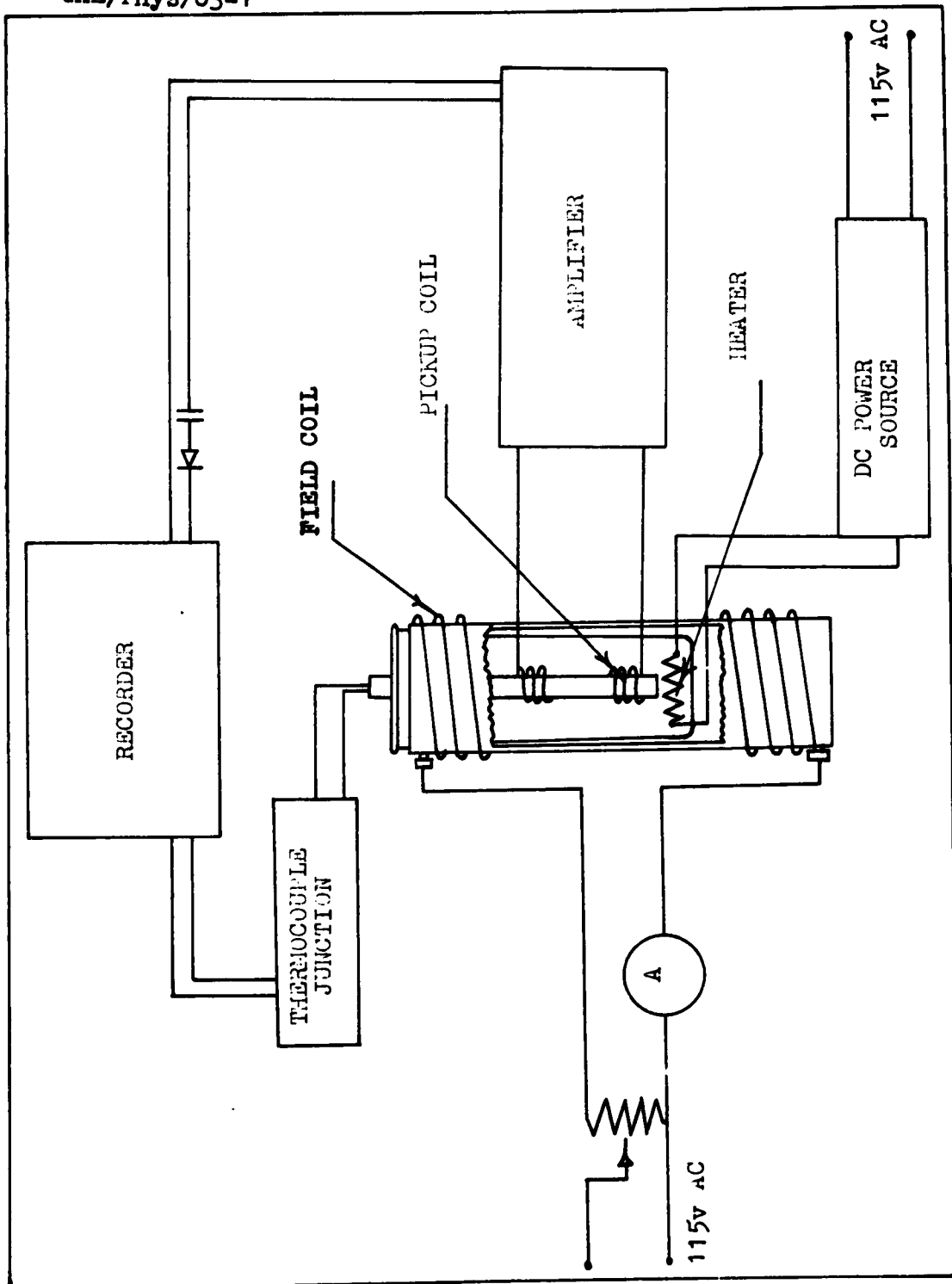


Fig. 14. Solenoid and dewar complex used in measuring Curie temperatures.



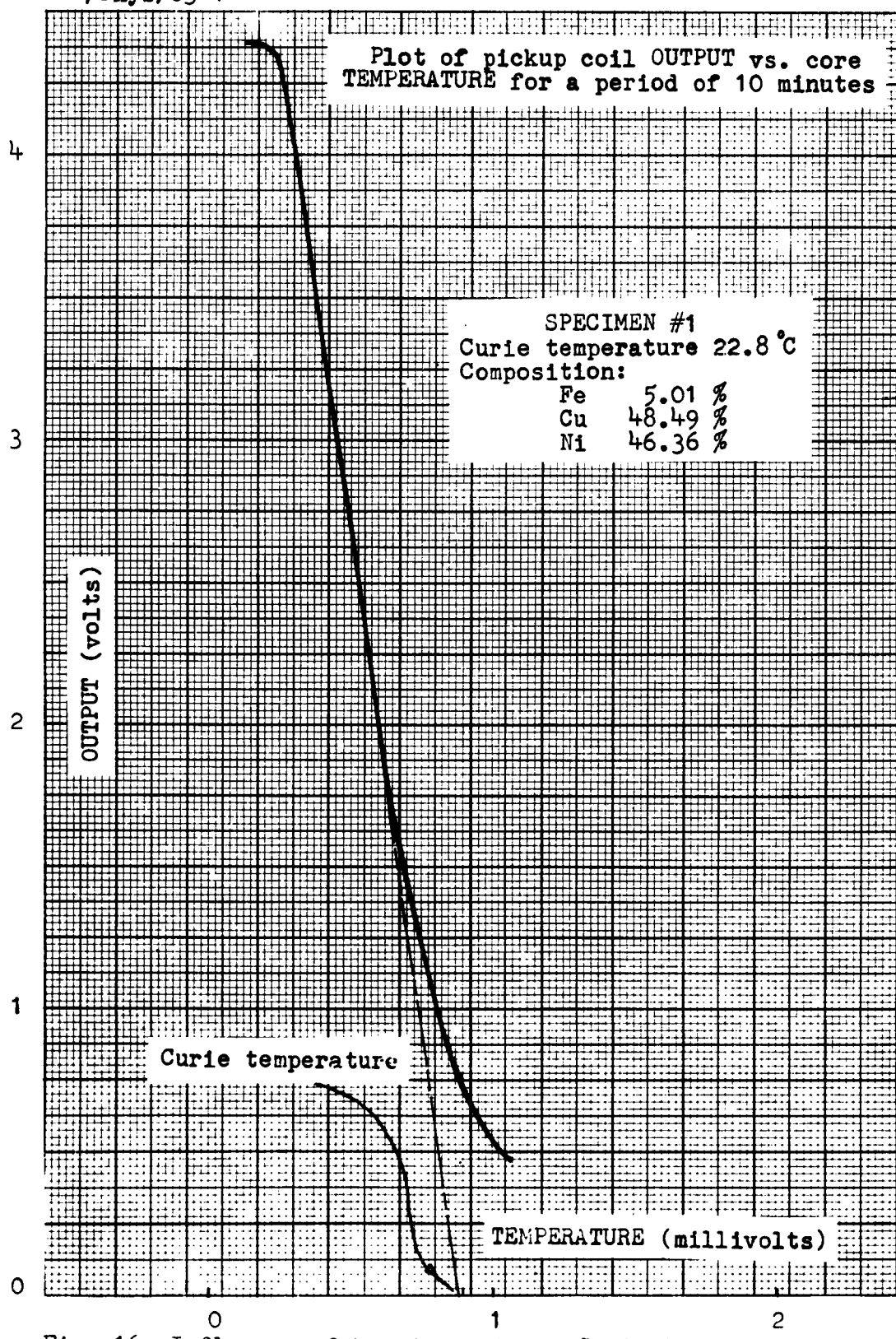


Fig. 16. Influence of heating rate on Curie temperature.

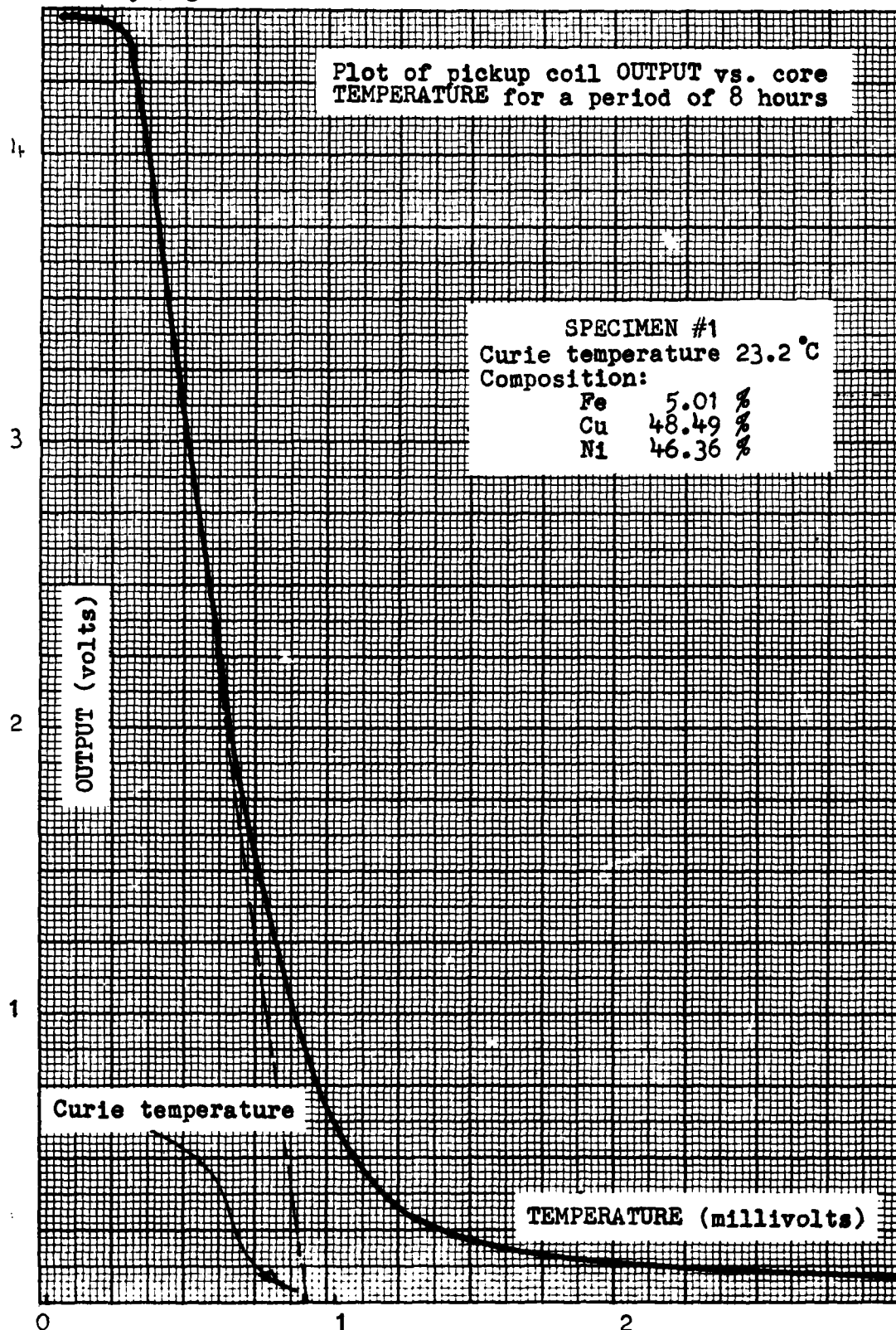


Fig. 17. Influence of heating rate on Curie temperature.

junction were used. A comparison shows little influence of the heating rate on the extrapolated value of the Curie temperature.

The procedure of plotting pickup coil output (volts) vs. Ni-Cu-Fe core temperature (millivolts) was repeated for 90 of the 105 Ni-Cu-Fe alloys prepared. Curie temperatures could not be determined for 15 specimens because the temperatures involved were beyond the capabilities of the apparatus. A mere sampling of the range of Curie temperatures measured is shown in Figures 18 thru 28, Appendix F. The graphs used to determine the Curie temperatures of the Ni-Cu-Fe specimens show a decrease in pickup coil output near the Curie temperature of the Core. The Curie temperature is determined by extrapolation of the steepest slope, as shown. Of particular interest is the range of Curie temperatures (-67.6 °C to 137.5 °C) associated with a 2% change in Fe. In addition, the per cent compositions do not total 100% showing the presence of some foreign material. The tabulated data of Fig. 29, Appendix G, presents the data obtained from the 45 alloys regarded as the most reliable. Results of the Curie temperature measurements are presented in the next chapter.

#### Measurement of Initial Permeability

Following the measurement of Curie temperature vs. alloy composition for 90 samples, the next step was to measure in-

initial permeability. The purpose of this section is to present the experimental procedure used to investigate the temperature dependence of the initial permeability. Two methods of measurement were attempted. The first attempt was unsuccessful but did yield valuable insight into the problems of low field  $H$  measurements. The second attempt to measure initial permeability was partially successful but limited to a single Ni-Cu-Fe toroid. Since the experimental apparatus was quite simple, a single schematic for a toroidal specimen is given in Fig. 30. Variations of this apparatus are described for each method of measuring initial permeability.

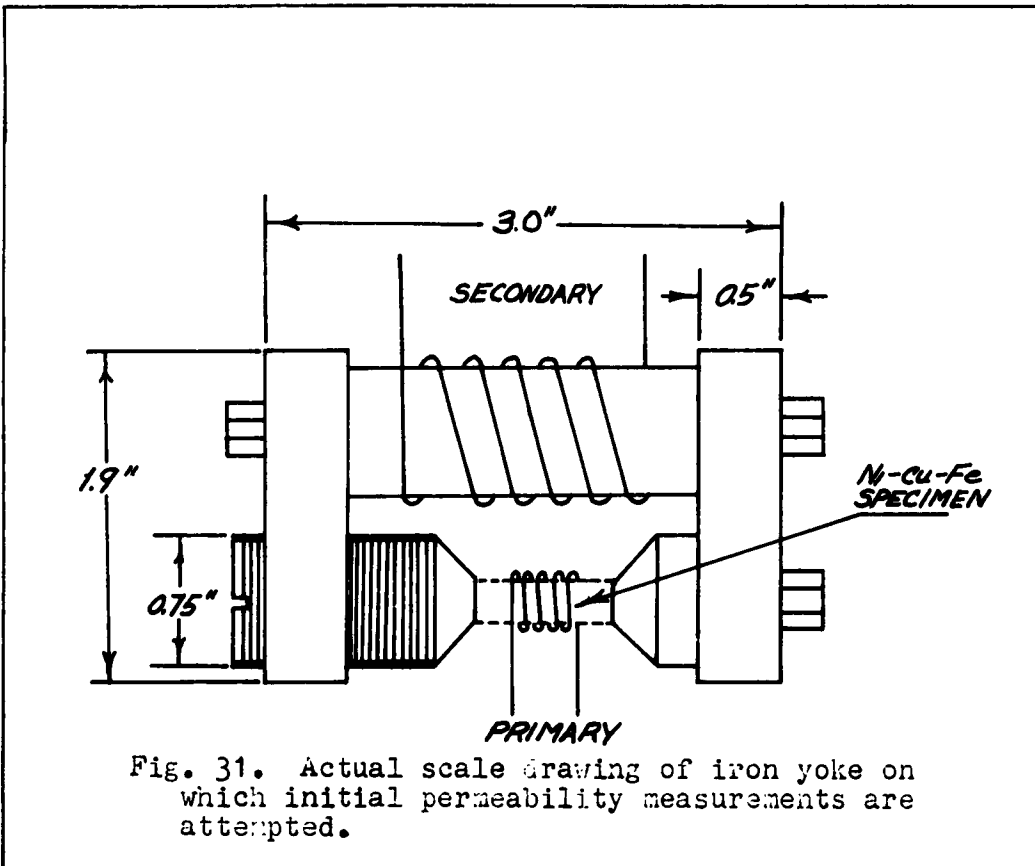
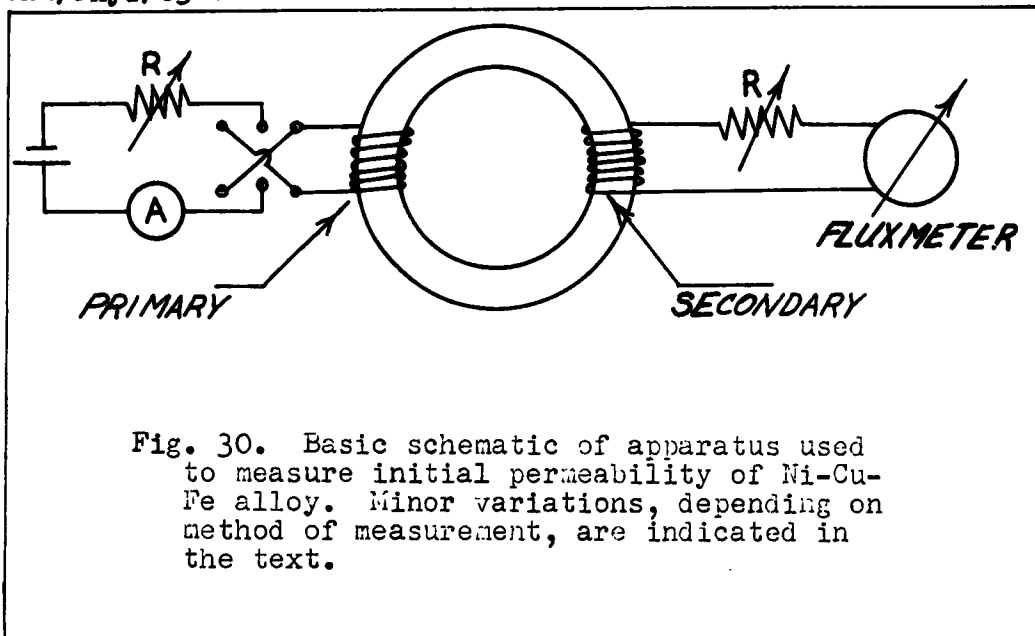
The general procedure is to make the magnetic field intensity  $H$  a small fraction of the value of  $H$  causing saturation of the magnetic induction  $B$  for the Ni-Cu-Fe alloys. This procedure approximates the initial permeability range of the magnetization curve. The fluxmeter measures a change in flux  $\Delta\phi$  equal to,

$$\Delta\phi = A \Delta B \quad (5)$$

and from  $B = \mu H$ , the expression for the change in flux becomes,

$$\Delta\phi = \mu A \Delta H \quad (6)$$

and since the total change of the magnetic field intensity  $\Delta H$  is constant upon reversal of the current in the primary,



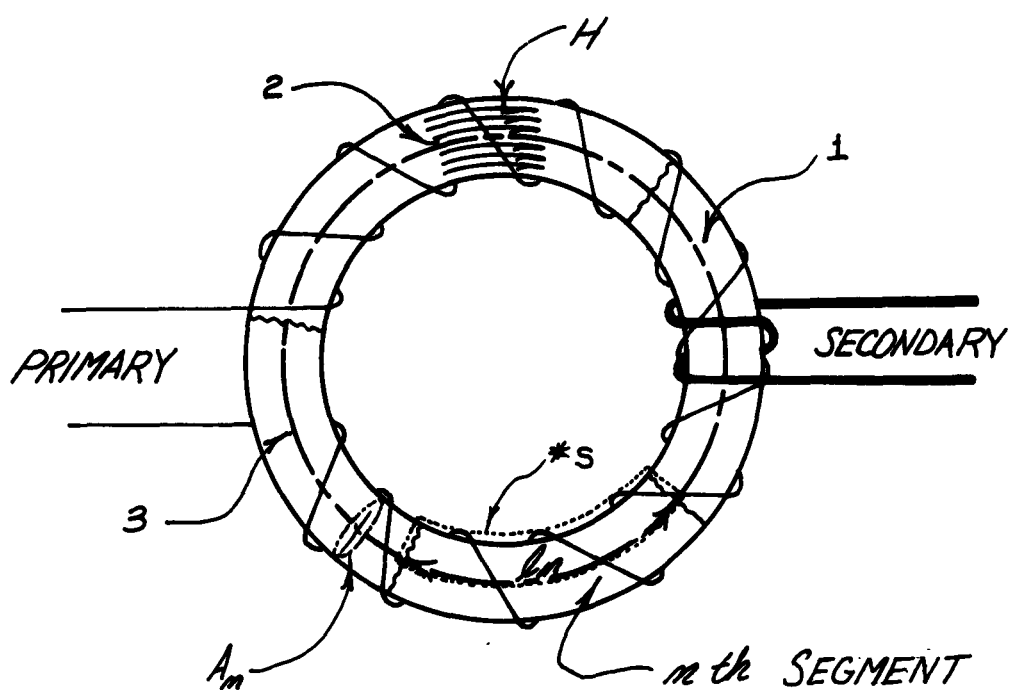
the fluxmeter measures a change in flux directly proportional to the permeability  $\mu$ . For small values of  $H$ , the permeability  $\mu$  can be assumed to be the initial permeability  $\mu_i$ .

The first attempt to measure  $\mu_i$  for the Ni-Cu-Fe rods involved the design of an iron yoke. The purpose of the iron yoke was to provide a high permeability medium for the flux induced in the Ni-Cu-Fe rod. The yoke also provided a reasonable area on which many turns of a secondary coil could be wound. An actual scale drawing of the yoke is shown in Fig. 31. In addition, the yoke overcomes the demagnetizing effect of the short Ni-Cu-Fe rod (Ref 3:10) and together, the yoke and the rod can be treated as a compound toroid. For the compound toroid shown in Fig. 32, consider that it consists of 1, 2, 3, . . . . ,  $n$  segments with varying properties. It can be assumed that the flux  $\phi$  is constant for any cross section or,

$$\phi = B_m A_m = \text{CONSTANT} \quad (7)$$

where  $B_m$  is the magnetic induction and  $A_m$  is the cross sectional area for the  $n$ th segment. From the expression for the permeability  $\mu_m$  of the  $n$ th section it follows that,

$$H_m = \frac{\phi}{\mu_m A_m} \quad (8)$$



$*S$  Indicates the area under consideration

$H$  = magnetic field intensity

$l_m$  = mean length of segment

$A_m$  = area of cross section

$N_p$  = number of turns in primary

$N_s$  = number of turns in secondary

Fig. 32. The compound toroid used as the mathematical model for the iron yoke and the Ni-Cu-Fe rod.

From Maxwell's law for the magnetomotive force (Ref 10:5-24),

$$\oint \vec{H} \cdot d\vec{l} = \frac{4\pi}{10} N_p \iint \vec{J} \cdot d\vec{S} = 0.4\pi N_p I_p \quad (9)$$

where  $d\vec{l}$  is an incremental length of the arbitrary path bounding the area  $S$  under consideration,  $N_p$  is the number of turns in the primary,  $\vec{J}$  is the current density in the primary,  $d\vec{S}$  is an element of area  $S$  enclosed by the arbitrary path  $\vec{l}$  and  $I_p$  is the current in the primary. Since  $H_m$  is constant for the  $n$ th section and entirely confined to the toroid, the line integral of the magnetic field reduces to,

$$\oint \vec{H}_m \cdot d\vec{l}_m = \sum_m H_m l_m = 0.4\pi N_p I_p \quad (10)$$

Combining (8) and (10) gives the expression for the flux,

$$\phi = \frac{0.4\pi N_p I_p}{\frac{l_1}{\mu_1 A_1} + \frac{l_2}{\mu_2 A_2} + \dots + \frac{l_m}{\mu_m A_m}} \quad (11)$$

For the case of the yoke (subscript  $y$ ) and the Ni-Cu-Fe rod (subscript  $s$ ) equation (11) takes the form,

$$\phi = \frac{0.4\pi N_p I_p}{\frac{l_s}{\mu_s A_s} + \frac{l_y}{\mu_y A_y}} \quad (12)$$

where the right hand term in the denominator expresses the influence of the yoke reluctance. In addition, this term is constant for iron since significant changes in  $\mu$  do not occur until its Curie temperature of  $770^{\circ}\text{C}$  is approach-

ed. This temperature is well above any of the Curie temperatures of the Ni-Cu-Fe alloys to be measured.

The experimental apparatus shown in Fig. 30 was used for the iron yoke and the Ni-Cu-Fe specimen. The yoke and specimen were placed in a dewar containing the nichrome heater and the dewar was filled with water. A copper-constantan thermocouple had been attached to the specimen and output was read on a voltmeter. Calculations used to determine the initial permeability range of the Ni-Cu-Fe alloys pointedly showed the limitations on this method of measuring  $\mu_i$ . An upper limit for  $\mu$  was determined by using saturation conditions for monel metal as an approximation of the saturation conditions for the Ni-Cu-Fe alloys (Ref 3:310). It was found that  $B_{SAT} = 1,000$  gauss and using reasonable values for the parameters involved with the iron yoke and the Ni-Cu-Fe rod, the saturation flux was found to be,

$$\phi_{SAT} = B_{SAT} A_s = (1,000) (.3) = 300 \text{ maxwells}$$

giving,

$$\Delta\phi_{SAT} = \Delta B_{SAT} A_s = 2B_{SAT} A_s = 600 \text{ maxwells}$$

upon reversal of the field  $H_{SAT}$ . For a desired deflection  $\checkmark$  of the fluxmeter equal to 60 divisions, the number of

turns required in the secondary coil  $N_s$  were found to be,

$$N_s = \frac{S}{\Delta \phi} = \frac{(60)(5,000)}{600} = 500 \text{ turns}$$

where  $S$  is the sensitivity of the fluxmeter. Therefore, 500 turns on the secondary would be reasonable if  $B = 1,000$  gauss. However, for initial permeability measurements one tenth of  $B_{SAT}$  was arbitrarily selected and from Fig. 4, an initial permeability of 4,000 gauss/oersted is seen to be a representative value for the Ni-Cu-Fe alloys. Using a value for  $\phi = 30$  maxwells gave  $N_s = 5,000$  turns. The requirement of 5,000 turns for the secondary could not be matched to the 15 ohm external resistance required for the fluxmeter. For this reason meaningful measurements of initial permeability were not possible. However, this attempt to measure initial permeability did point out the considerations that must be made when using a yoke.

A second attempt to measure  $\mu_i$  was made by substituting an integrating digital voltmeter for the fluxmeter. This instrument gives a highly sensitive integration of voltage over a short period of time and therefore behaves like a fluxmeter. Measurements were made on a small Ni-Cu-Fe toroid. The toroid was 1.6 cm in diameter with a cross sectional area of 0.12 cm. A single turn primary and a 300 turn secondary were used. First a magnetization curve was

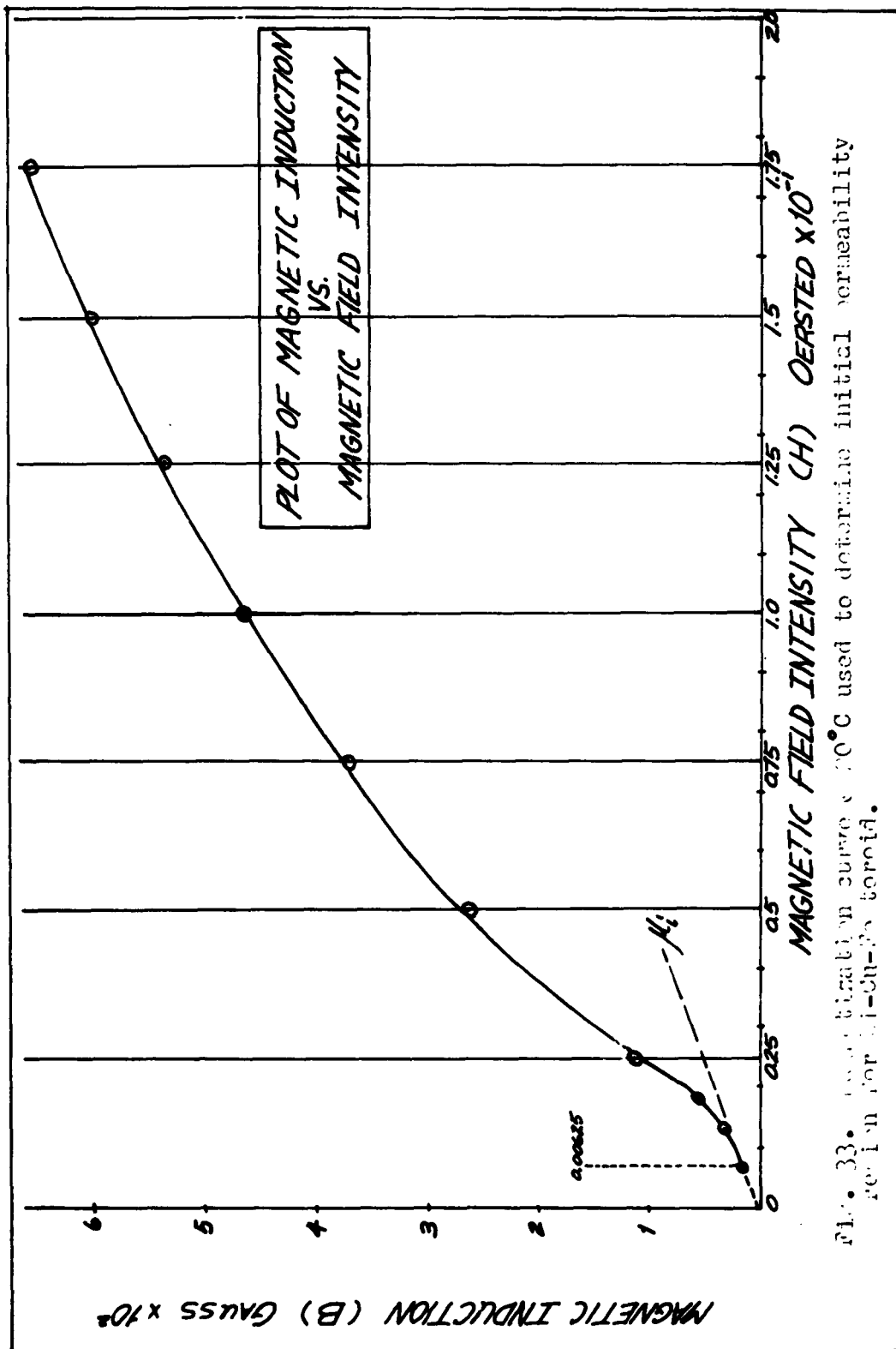


Fig. 33. Magnetization curve at 20°C used to determine initial permeability of iron in Cu-Pt, garnet.

GAE/Phys/63-1

plotted at room temperature to get a value of  $H$  in the initial permeability range (Fig. 33). The value of  $H$  used was 0.00625 oersted. The toroid was placed in a glass dewar with water and the nichrome heater. Temperature measurements were made with a mercury thermometer having a sensitivity of  $0.1^{\circ}\text{C}$ . For this case, a thermometer was adequate since sufficient time must be allowed between measurements to avoid thermoelectric noise to the integrating digital voltmeter. A plot of magnetic induction vs. temperature is given in the next chapter. A peak initial permeability of 2,670 gauss/oersted was obtained for the toroid with a Curie temperature of  $58.9^{\circ}\text{C}$ .

#### IV. Discussion of Results and Conclusions

The purpose of this chapter is to discuss the experimental results obtained during the course of this investigation. The plan is to present the results by an analysis of the preparation of the Ni-Cu-Fe alloys, measurement of Curie temperature, and measurement of initial permeability. Appropriate recommendations are included in each section.

##### Analysis of Alloy Preparation

The method of preparation of the Ni-Cu-Fe alloys is extremely important in determining the final magnetic characteristics. Curie temperature and magnetic induction are especially sensitive to impurities (Ref 3:19). Strain, temperature, crystal structure, and crystal orientation affect the initial permeability (Ref 3:15). Obviously, very pure and consistent melts are necessary to produce reliable data.

Both the levitation furnace and the induction furnace had not been used extensively at the beginning of this investigation. Concurrently, modifications were necessary in order to increase their reliability and usefulness. This meant that the quality of the melts produced could not be predicted. As a result, many of the anomalies found after measuring the Curie temperatures of the Ni-Cu-Fe alloys could have been due to impurities introduced during melting. However, since the levitation furnace was evacuated to 50

microns and melting accomplished in a pure Argon atmosphere, any impurities in the melts were more likely present before melting. Oxygen contamination of the metal powders indicates the need for very pure raw materials. The effect of impurities is discussed in conjunction with the analysis of the Curie temperature measurements.

One of the important, but secondary accomplishments of this investigation was the pressing of pure metals into small cylinders and successful use of a levitation device to produce melts. Coarse grain powders were found to be the most convenient to weigh and are capable of being pressed to high densities. The design of a large glove-box containing a small hydraulic hand press and balance in an inert atmosphere would permit extremely pure melts to be made. In this way, the problem of oxygen contamination is avoided.

Even after the elimination of the crucible by levitation melting, the use of very pure metals, and melting in a pure Argon atmosphere, there remain areas of investigation. Of primary concern is the question of homogeneity of the specimen. The field of the levitation device appears to provide an extremely vigorous stirring action and mechanical mixing of the nickel, copper, and iron should be complete. If the specimen is not homogeneous, the annealing procedure allows thorough diffusion if a high enough temperature is maintained for a sufficient time. The previous assumption that the

vigorous mixing action of the levitation field provided homogeneity was likely erroneous. This postulation is further supported by small discrepancies in the Curie temperatures of specimens from different melts but prepared with identical compositions. The procedure of machining the specimens before annealing likely caused an appreciable change in total percentage of Ni-Cu-Fe, accounting for the discrepancy in Curie temperature. Final chemical analysis showed that composition changes had taken place. In addition, a final series of 8 alloys were melted in an attempt to plot the 46°C Curie temperature line on the ternary diagram. The compositions of these alloys were based on previous Curie temperature measurements and assumed compositions, since chemical analysis had not yet been performed. However, machining was not done until after the annealing process. The resulting Curie temperatures of these specimens were higher (approx. 58°C) and chemical analysis showed greater Fe content. Homogeneity must have been achieved during the 24 hour annealing period, as indicated by the smoothness of the Curie temperature curves of pickup coil output vs. core temperature.

Figure 34 is shown because of its different characteristics. Repeated runs did not change the appearance of the Curie temperature curve. The non-linear portion of the curve suggests inhomogeneity or the presence of a second phase.

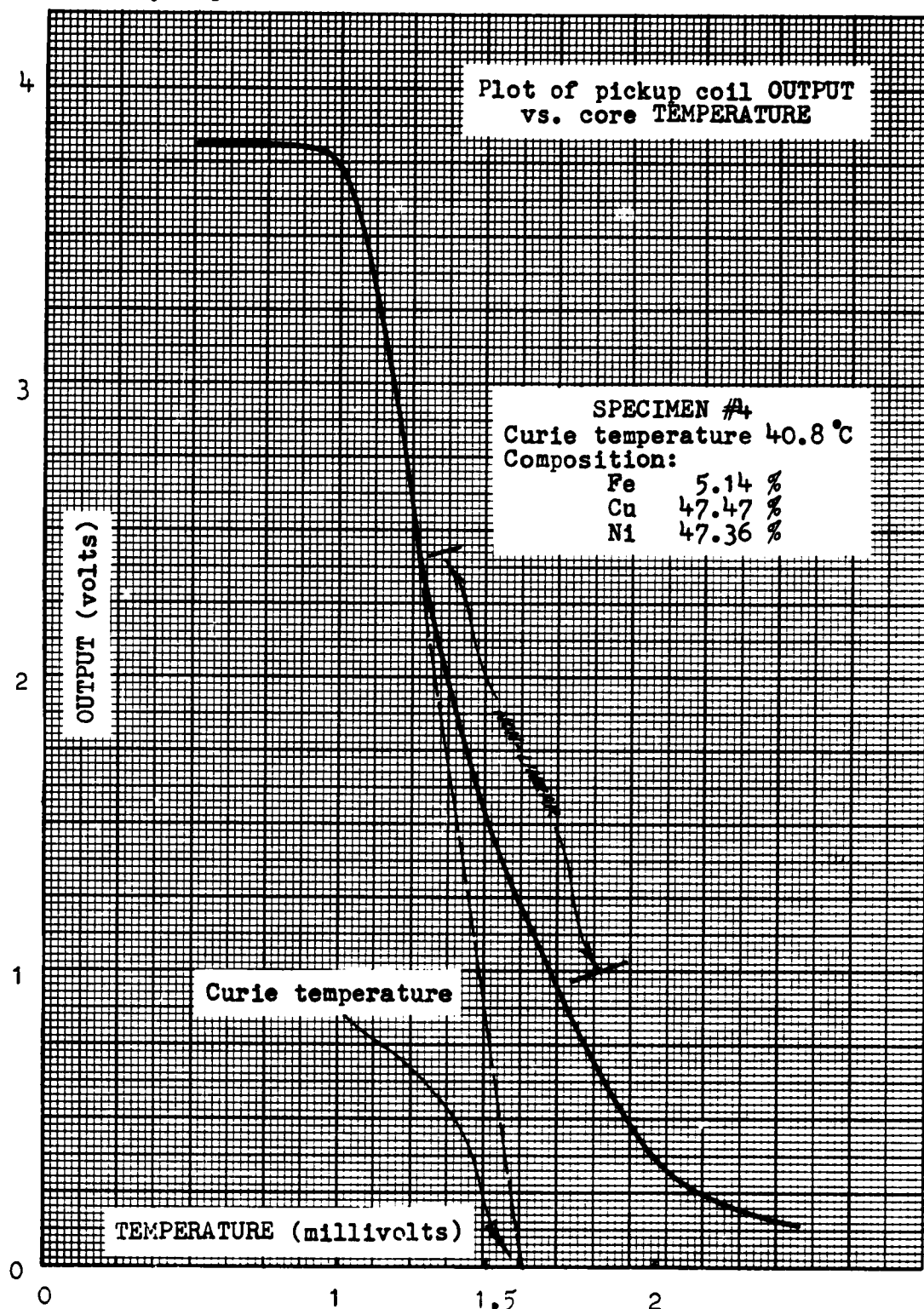


Fig. 3<sup>4</sup>. Measurement of Curie temperature of Ni-Cu-Fe rod. Non-linearity of curve indicates the presence of two phases or an inhomogeneous specimen.

An x-ray examination could have been used to determine if a second phase did exist. The non-linear portion of this curve is also characteristic of the normal curve for ferrite (Ref 8: 315), suggesting the presence of an iron oxide. However, since none of the other Curie temperature curves showed the characteristics of Fig. 34, it was assumed at this point that the 24 hour homogenizing period was sufficient and that quenching at 625°C was adequate in maintaining a single phase.

The final chemical analysis given in the tabulated data of Fig. 29, Appendix G, indicated impurities in the Ni-Cu-Fe alloys varying from 0.7% to 0.01% by weight. In general, the chemical analysis compared favorably with the per cent compositions prepared in the laboratory. A loss in weight during melting was subsequently reflected by a change in composition in the chemical analysis. Of particular interest were the alloys showing a total percentage of Ni-Cu-Fe of approximately 99.99%. In the case of these very pure alloys, the individual percentages were nearly those of the original compositions. In addition, the pure alloys showed little or no change in total weight during the preparation of the alloy.

#### Analysis of Curie Temperature Measurements

The primary accomplishment of this investigation was mapping the area shown in Fig. 35. From 105 Ni-Cu-Fe alloys produced, 45 were used to plot the Curie temperature lines shown on the ternary diagram. These alloys were selected

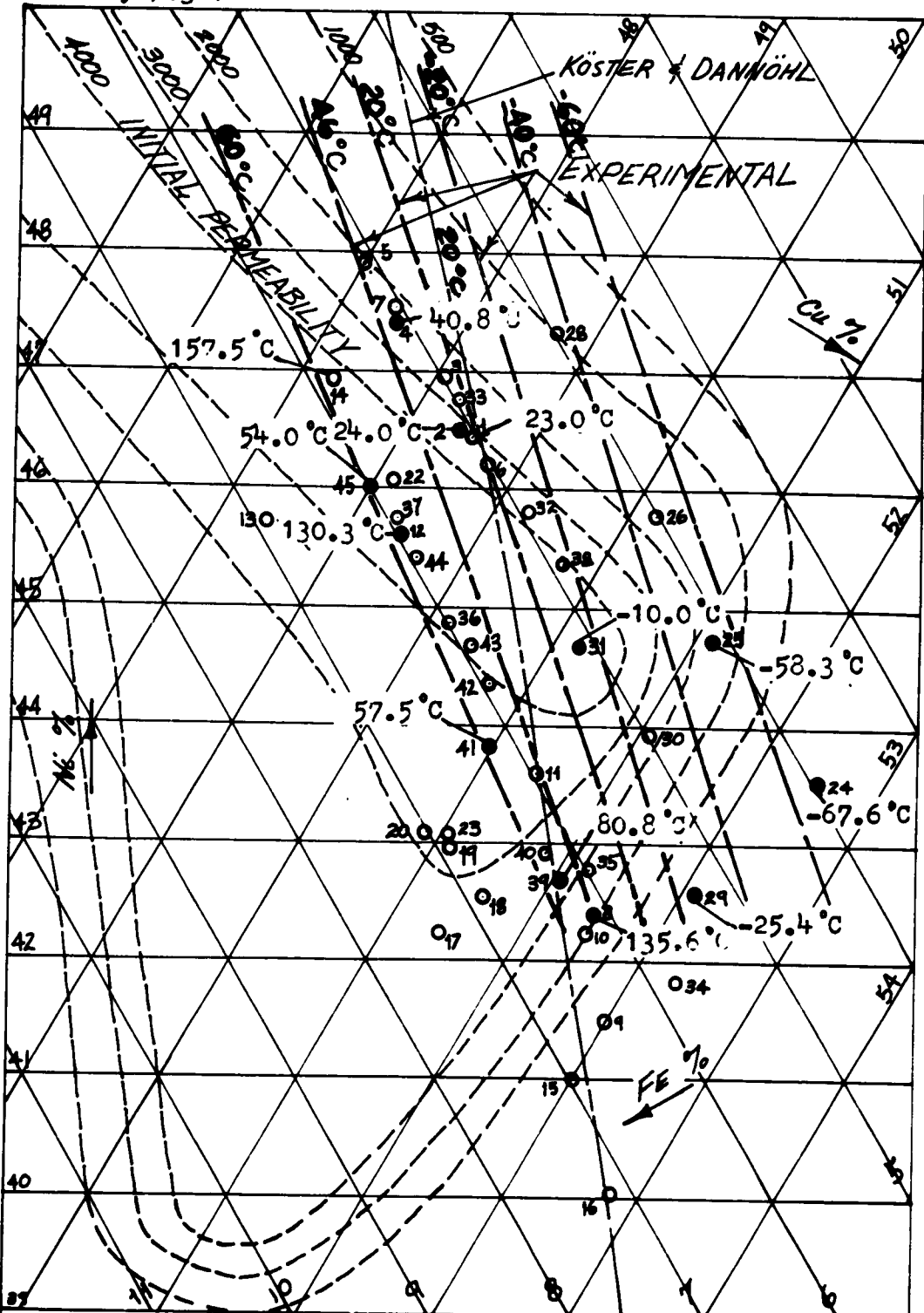


Fig. 35. Enlarged view of area investigated of Ni-Cu-Fe ternary showing results of Curie temperature measurements. Temperatures are indicated for high purity alloys.

from results of the chemical analysis. The heavier dashed lines are estimates of lines of constant Curie temperature from  $-60^{\circ}\text{C}$  to  $+60^{\circ}\text{C}$ . The primary data points used to estimate these lines are indicated by solid black dots. The black dots also indicate the very pure Ni-Cu-Fe alloys mentioned earlier. In addition, the individual Curie temperatures are indicated for the very pure alloys. Lines of initial permeability determined by Von Auwers and Neumann and the  $20^{\circ}\text{C}$  Curie temperature line determined by Koster and Dannohl are indicated for use as a reference to Fig. 4. The remainder of the 45 data points were also plotted and used to substantiate the estimated constant Curie temperature lines. Since the composition of the alloys represented by these secondary data points does not total 100%, the method used to plot the point was to form a small triangle with the individual percentages from the chemical analysis and estimate placement of the data point. Placement of the data point was midway and directly on the Fe side of the triangle. This procedure was used because the accuracy requested for chemical analysis of the Fe was tenfold of that requested for the Ni and Cu. Figure 29, Appendix G, gives the tabulated results of the Curie temperature measurements and the chemical analysis. Correlation between the  $20^{\circ}\text{C}$  line given by Koster and Dannohl and the  $20^{\circ}\text{C}$  line determined by this investigation is shown on Fig. 35. Also shown is

the 46 °C Curie temperature line. A sampling of the Curie temperature curves is shown in Figs. 18 thru 28, Appendix F.

The higher Curie temperature region on the ternary diagram indicates poor agreement between data points. To the left of the estimated 20 °C line, several points with very high Curie temperatures are indicated. In addition, this large temperature difference is shown between very pure alloys. This temperature difference strongly indicates that quenching at 625 °C caused precipitation of the  $\gamma$  +  $\gamma_1$  phases for several melts. As a result, the individual Curie temperatures of each phase could be quite different. In the event that one of the phases was non-magnetic or had a very low Curie temperature, only the highest Curie temperature would have been recorded since the Ni-Cu-Fe rod was placed in the specimen holder and if a net output was indicated, the temperature was increased. The high Curie temperatures could be those of a single phase having an individual composition in the higher Curie temperature range. Subsequent chemical analysis would reflect a composition based on both phases. An x-ray study of the phase equilibrium lines by Bradley, Cox and Goldschmidt indicates that quenching at 700-750 °C would have eliminated the two phase problem (Ref 4:189-201). Another possible explanation for the high Curie temperatures is the reduction in Ni or Cu by a chemical reaction with some impurity. A 2% reduction in

Ni and a 1% reduction in Cu would account for the higher Curie temperatures. Since the chemical analysis of the Ni and Cu was done electrolytically, dissociation of the Ni and Cu would account for the final chemical analysis showing the original composition.

On the other hand, the region of Fig. 35 to the right of the estimated  $20^{\circ}\text{C}$  line shows very good agreement between pure alloys. Slight differences between the Curie temperatures of those alloys whose chemical analysis showed the presence of impurities could be due to the actual measurement of Curie temperature. Very small amounts of impurities (0.02%) can cause a marked change in the magnetic induction (Ref 3:19). Since the output of the pickup coil used to measure Curie temperature is a function of the magnetic induction, the presence of an impurity causing  $B$  to change would result in a different slope of the curve in general. The change in the slope of the output vs. temperature curve is due to the fact that the effect of the impurity on  $B$  is not linear. Thus the extrapolated Curie temperature could be in error by several degrees.

An attempt to verify the validity of the Curie temperature measurements was made by melting two cylinders of identical composition and casting in the shape of a rod and a disc. The disc was machined into a toroid and wound with a secondary coil. A comparison of these two specimens is

given in Figs. 27 and 28, Appendix F. The small difference in Curie temperature is accredited to a second melting of the toroid before a proper disc was produced. The toroidal curve is interesting for several reasons. First it presents the classical magnetic induction vs. temperature curve. Secondly, from the continual decrease in induction, it shows that all Curie temperature measurements were made with the specimens near saturation.

The Curie temperature measurements represent an exhaustive coverage of a small area of the entire Ni-Cu-Fe ternary. The 46°C Curie temperature line was estimated and mapping of the area provided more information on composition dependence of Curie temperature in the lower temperature range.

#### Analysis of Initial Permeability Measurements

The purpose of the initial permeability measurements was to investigate the temperature dependence of  $\mu_i$  and obtain the peak  $\mu_i$  for the heat treatment used. The problems of low field measurements are evident from the academic treatment given the iron yoke in the previous chapter.

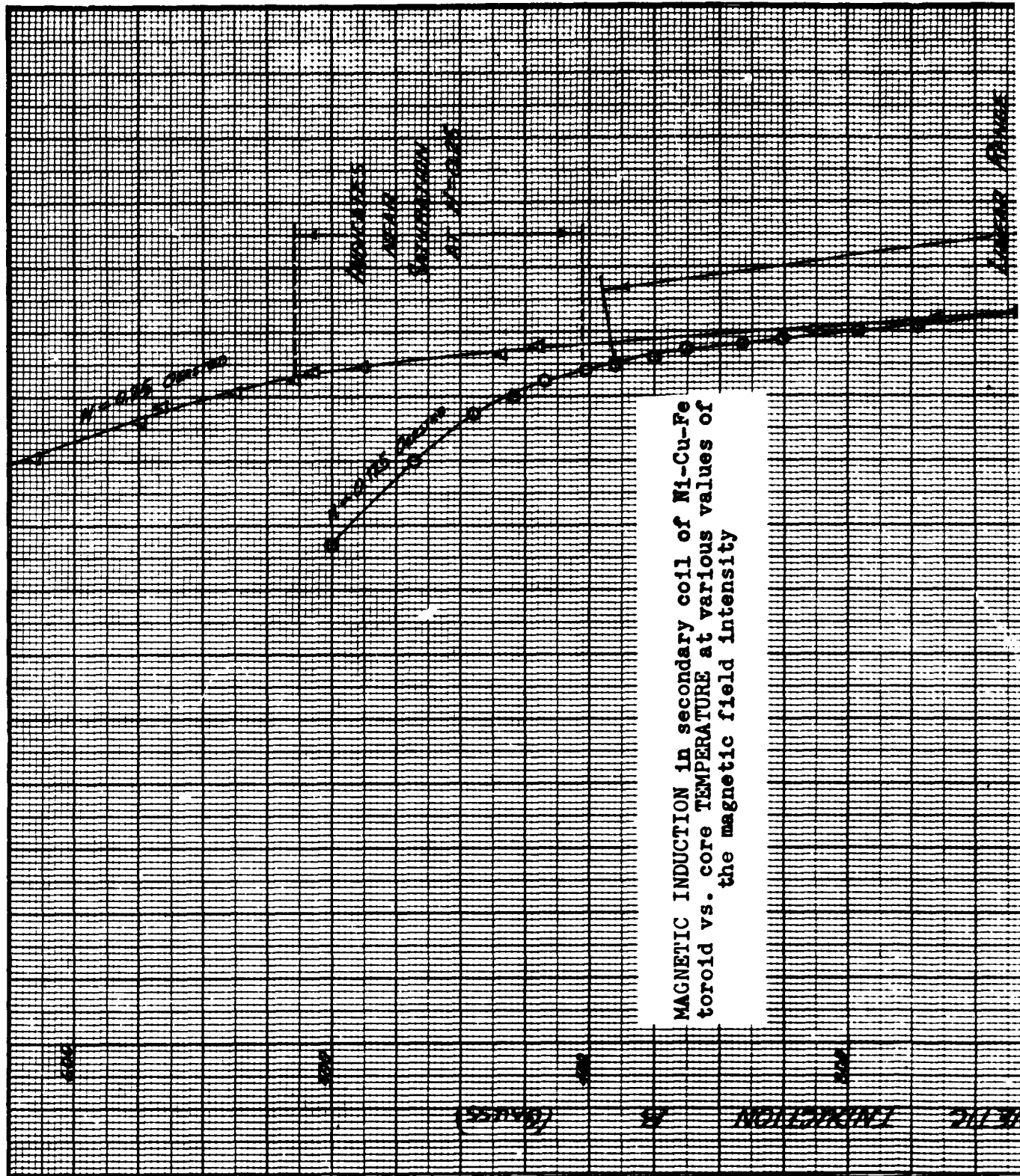
The iron yoke was an attempt to overcome the effect of the demagnetizing field on the magnetization curve of a short rod, resulting in a "sheared" curve (Ref 3:10). It was obvious from the magnetomotive force equation that the resulting flux is determined by the reluctance of the iron yoke.

A sensitive fluxmeter plus a precise measurement of the yoke reluctance are required if initial permeability is to be measured. The solution to this problem is to use a yoke material with an initial permeability much higher than the peak  $\mu_i$  for the Ni-Cu-Fe specimens, thus reversing the flux dependence of the two reluctance terms. Meaningful measurements could then be made on small rods with an integrating digital voltmeter.

Another course to pursue is to start with specimens in the form of toroids and use the integrating digital voltmeter to make the initial permeability measurements described in the previous chapter. A graph of magnetic induction  $B$  vs. temperature for the single Ni-Cu-Fe toroid is given in Fig. 36. Magnetic induction was plotted instead of  $\mu_i$  vs. temperature to show the effect of changing magnetic field strength  $H$ . The peak  $\mu_i$  is 2,670 gauss/oersted at  $H = 0.00625$  oersted. The value of  $H = 0.00625$  oersted is the lowest point measured on the magnetization curve and is in the initial permeability region. However, it appears that this value of  $H$  is the upper limit on  $\mu_i$  and also a practical lower limit on the integrating digital voltmeter. For this reason, the curve shows only a slight hump and does not show the theoretical shape desired. The lower limit on the integrating digital voltmeter can possibly be extended through the use of a triangular pulse generator. An oscil-

1

GAE/Phys/63-1



toroid vs. core TEMPERATURE at various values of  
the magnetic field intensity

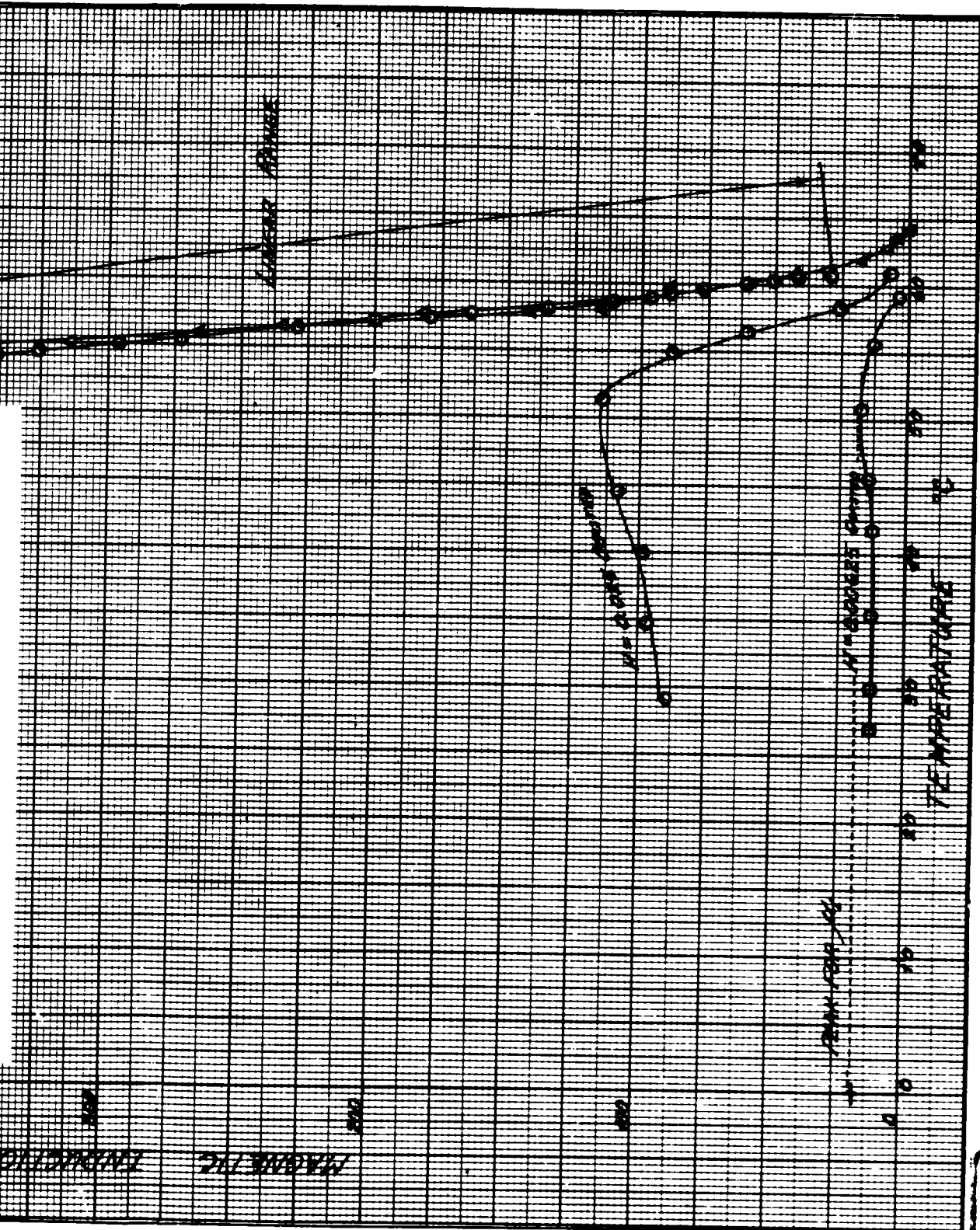


Fig. 36. Plot of magnetic induction  $B$  vs. temperature for  
Ni-Cu-Fe toroid.

lograph study showed that the pulse duration was extremely short upon reversal of the primary switch and thus beyond the optimum limits of the integrating digital voltmeter. The possibility exists that the integrating digital voltmeter is only capable of measuring the initial and final parts of the pulse, missing the peak of the pulse and accounting for the slight "hump" in  $B$ . The purpose of the pulse generator would be to replace the current reversing switch used in the primary of the toroid and allow a greater time for reversal. As a result, the integrating digital voltmeter would be able to integrate the entire pulse generated. A rough estimate can be made from the peak initial permeability as a representative figure of the maximum attainable by quenching in water at  $625^{\circ}\text{C}$ . This estimate is based upon the fact that the toroid composition falls in the maximum initial permeability range given by Von Auwers and Neumann. The entire range of initial permeability vs. composition and heat treatment is recommended for further investigation.

Extremely significant results are shown in Fig. 36 for higher values of  $H$ . It was found that the Ni-Cu-Fe alloy saturated at unusually low values of  $H$ . The small change in the linear portions of the curves  $H = 0.125$  oersted and  $H = 0.25$  oersted indicate that the toroid is near saturation. Of specific interest is the linear range of the

$H = 0.125$  oersted curve in relation to the 53-61 °C temperature range. This curve shows a linear change in magnetic induction of 50 gauss per degree Centigrade or a change in permeability of 400 gauss/oersted per degree Centigrade. In terms of a magnetic sensor of human body temperature, this means an extremely high sensitivity with a low power requirement. In addition, it is not necessary to use values of  $H$  in the initial permeability range because the Ni-Cu-Fe alloy saturates in very low fields. As a result, Fig. 36 definitely establishes the feasibility of the Ni-Cu-Fe alloy for use in sensing human body temperature.

#### Conclusions

The purpose of this study has been to investigate the magnetic properties of a series of Ni-Cu-Fe alloys. An efficient method of preparing alloys by levitation melting was developed. However, additional technique is required to insure higher purity alloys because of the narrow composition limits on Curie temperature for the Ni-Cu-Fe ternary. An efficient method of measuring Curie temperature for a large number of small rods was developed. Curie temperature measurements have provided more information on composition dependence. An upper limit on the field required to measure initial permeability has been established. An investigation of the inherent problems in DC measurement of initial permeability was also presented. Use of AC to measure initial

permeability would provide better data provided the eddy current problem could be overcome (Ref 7:141). One possible solution would be to have the Ni-Cu-Fe drawn into fine wire and bundled to form a core.

Conclusive experimental evidence was obtained which showed the feasibility of a Ni-Cu-Fe alloy for use as the active element of a sensor of human body temperature. The requirements of high sensitivity and low power are easily met without considering initial permeability.

This study provides data from which an optimum Ni-Cu-Fe alloy can be produced and meet the telemetry requirements of high sensitivity and low power necessary in a magnetic sensor of human body temperature. The problem remains to design and fabricate an actual device. The investigation of the magnetic properties of the Ni-Cu-Fe alloys is by no means complete. Additional alloys with a Curie temperature of  $43^{\circ}\text{C}$ , just above the upper limit of human body temperature, must be produced. The purity of these alloys must be an absolute certainty if the magnetic properties are to be investigated. Once these alloys have been produced, the entire range of heat treatment versus permeability must be investigated. In this manner an optimum alloy can be selected for use as the active element of a magnetic sensor of human body temperature. The highly sensitive temperature dependence of the Ni-Cu-Fe alloy makes it ideally suited to the field of magnetic thermometry.

Bibliography

1. Auwers, O. v., and H. Neumann. "Iron-nickel-copper alloys of high initial permeability." Wiss. Veroffentl. Siemens-Werken, 14:93-108 (1935).
2. Blalock, G. C. Principles of Electrical Engineering. New York: McGraw-Hill Inc., 1950.
3. Bozorth, R. M. Ferromagnetism. New York: D. Van Nostrand Co., Inc., 1951.
4. Bradley, A. J., W. F. Cox, and H. J. Goldschmidt. "An X-Ray Study of the Iron-Copper-Nickel Equilibrium Diagram at Various Temperatures." The Journal of the Institute of Metals, 67:189-201 (1941).
5. Christiansen, G. S., and P. H. Garrett. Structure and Change. San Francisco: W. H. Freeman & Co., 1960.
6. Koster, W., and W. Dannohl. "The copper-nickel-iron system." Zeitschrift fur Metallkunde, 27:220-226 (1935).
7. Moullin, E. B. The Principles of Electromagnetism. London: Amen House, 1932.
8. Richards, C. E., and A. C. Lynch. Soft Magnetic Materials For Telecommunications. New York: Interscience Publishers Inc., 1953.
9. Sears, F. W., and M. W. Zemansky. University Physics. Cambridge: Addison-Wesley Press, Inc., 1950.
10. Underhill, E. M. Permanent Magnet Handbook. Pittsburgh: Crucible Steel Company of America, 1957.
11. Vigoureux, P., and C. E. Webb. Principles of Electric and Magnetic Measurements. London: Blackie and Son Limited, 1936.

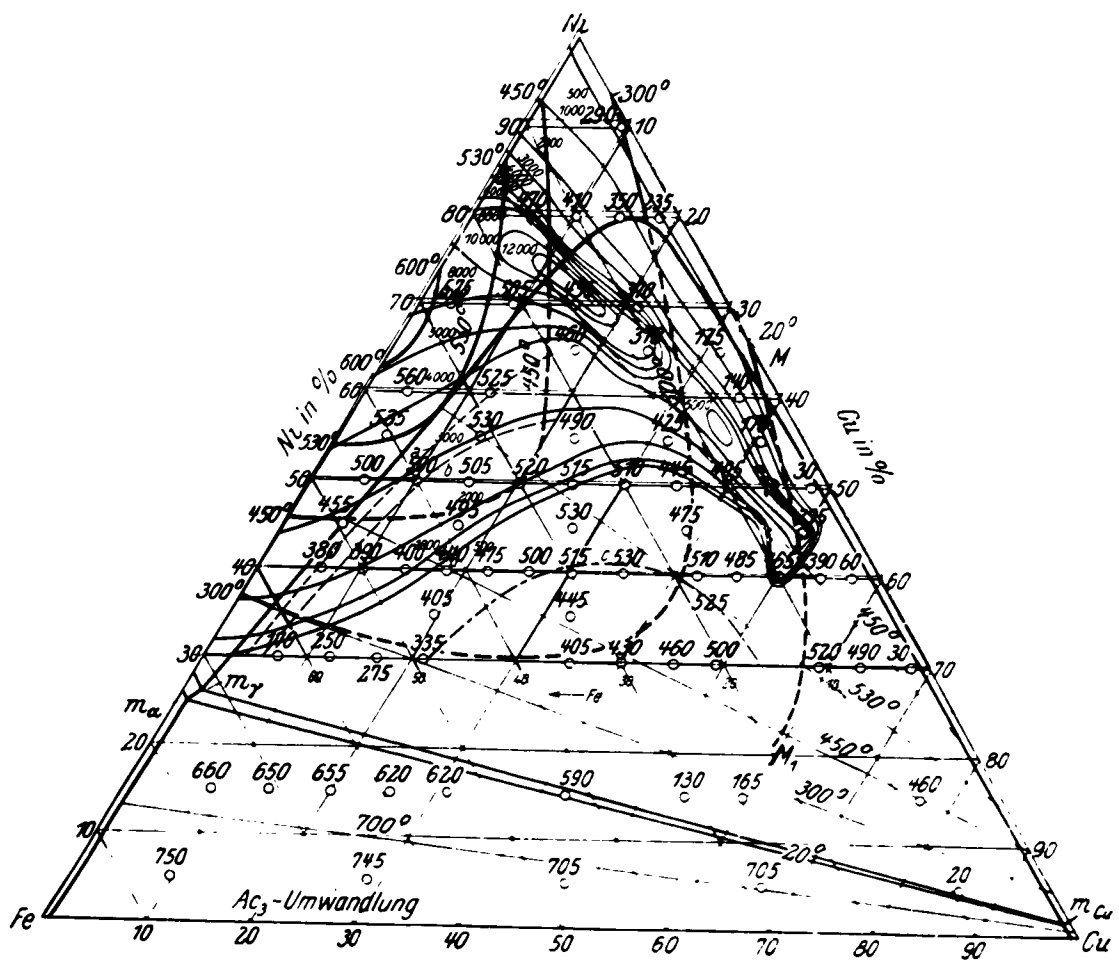


Fig. 5. Photograph of primary source material on Curie temperature and initial permeability after superpositioning.

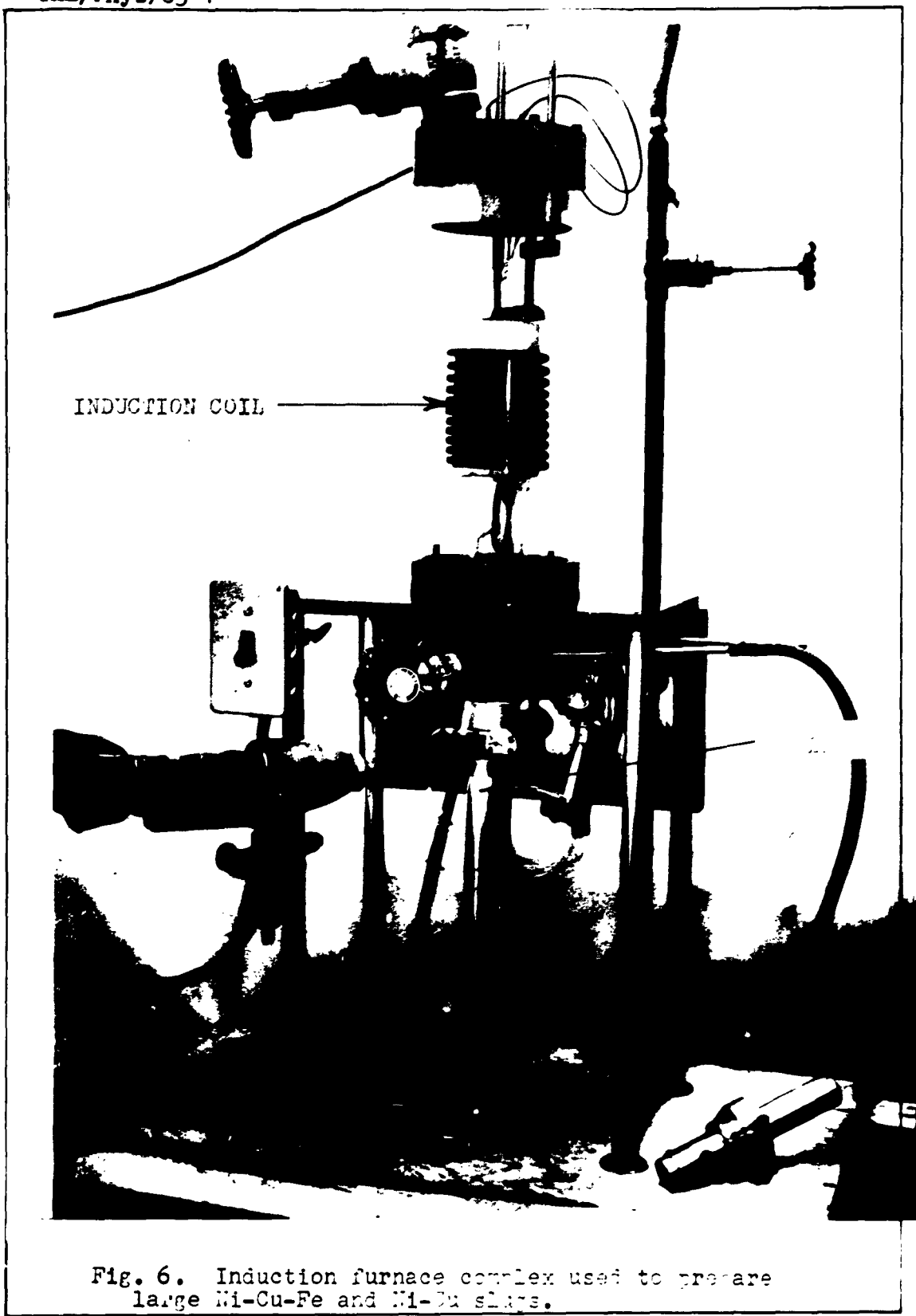


Fig. 6. Induction furnace complex used to prepare large Ni-Cu-Fe and Ni-Cu slugs.

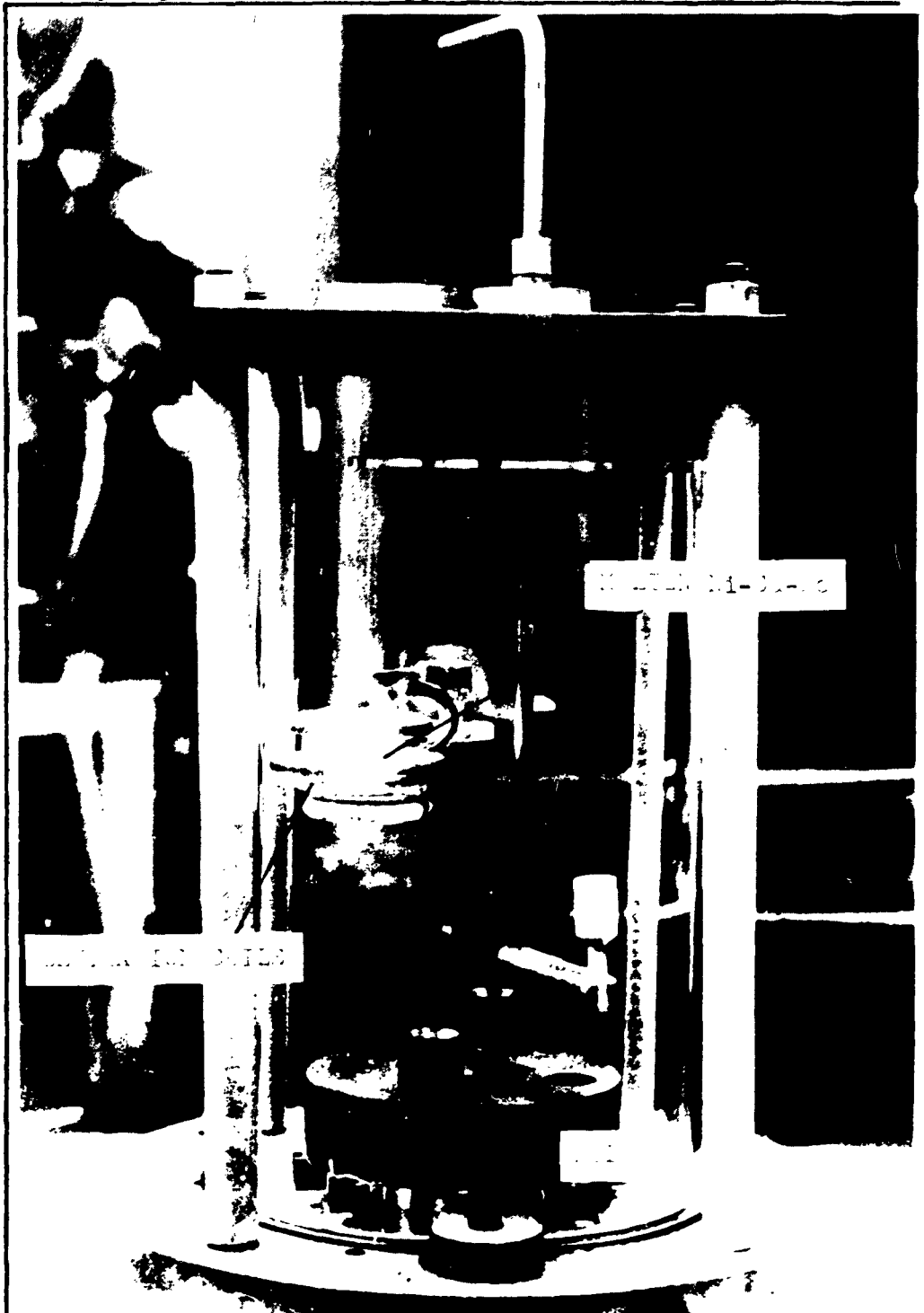


Fig. 8. Levitation furnace used to prepare Ni-Cu-Fe rods from pressed cylinders.



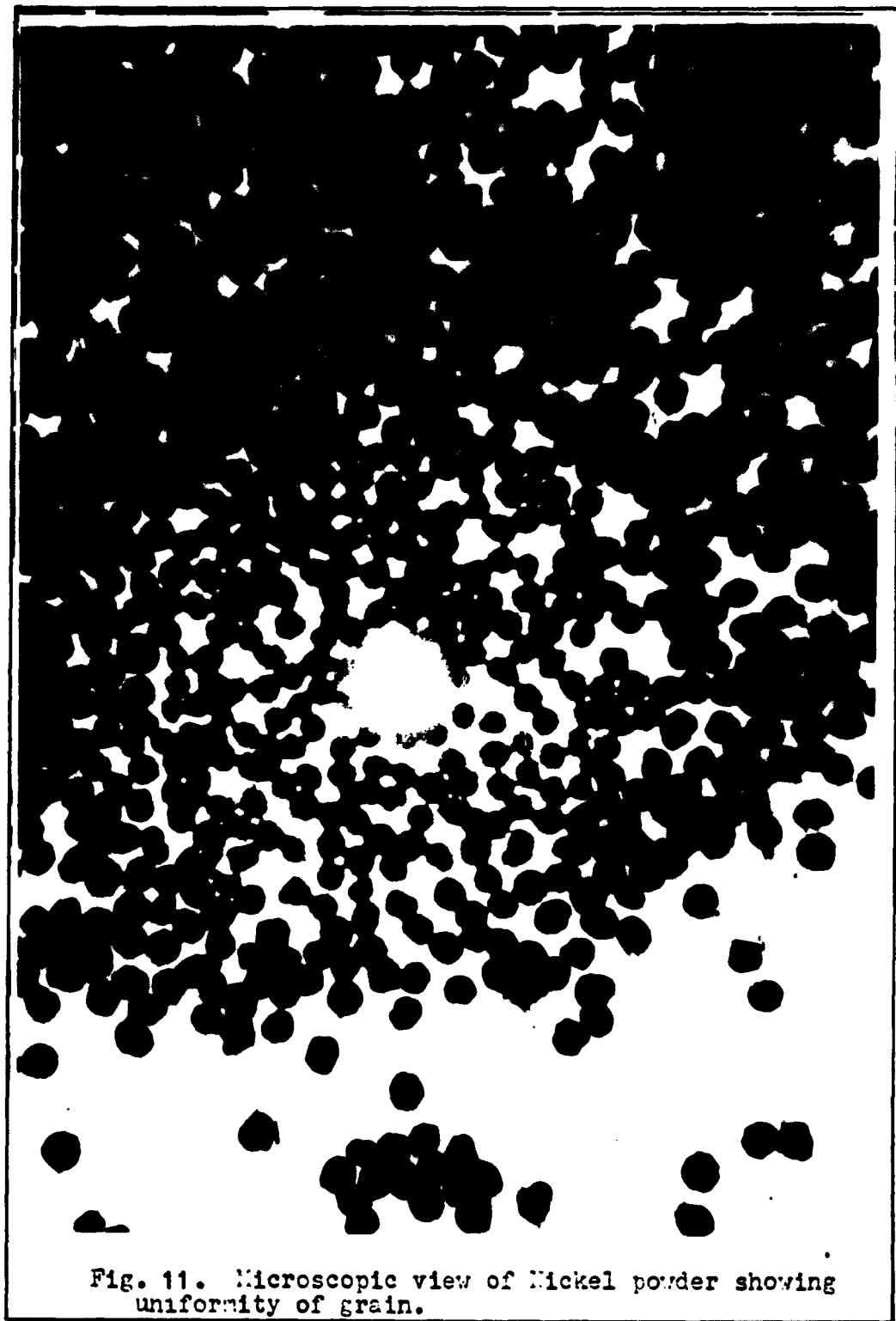


Fig. 11. Microscopic view of Nickel powder showing uniformity of grain.

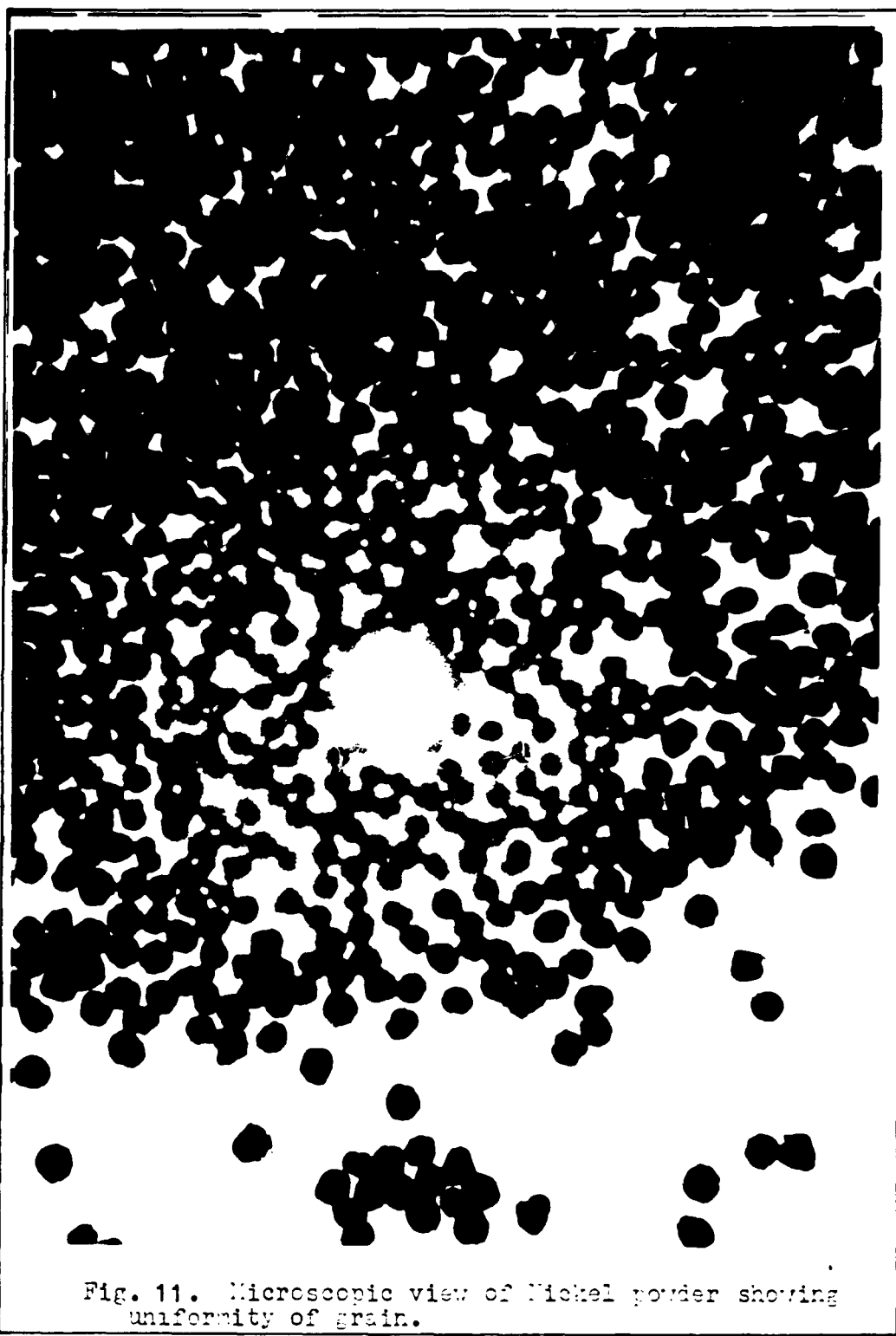


Fig. 11. Microscopic view of Nickel powder showing uniformity of grain.

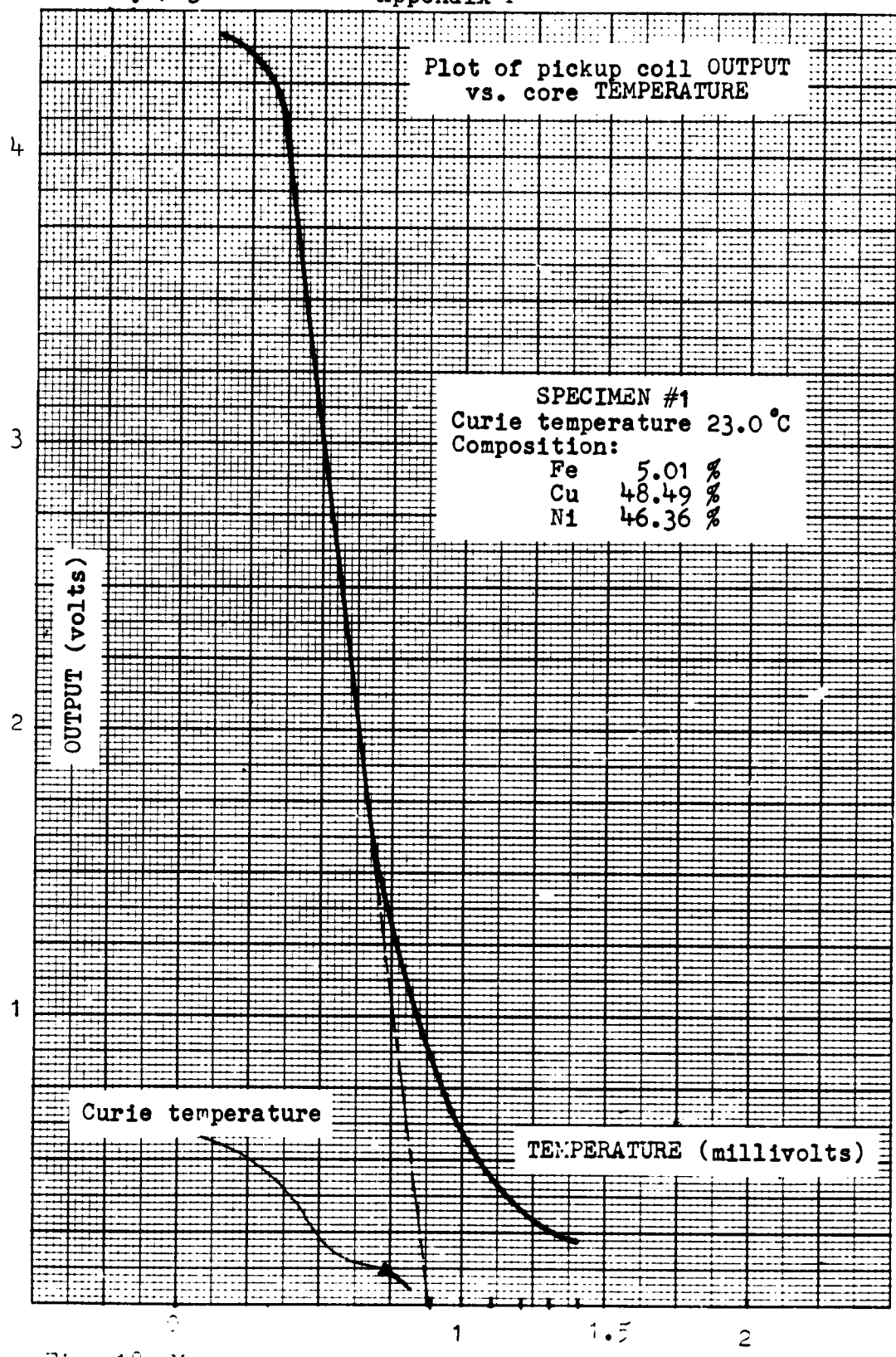


Fig. 18. Measurement of Curie temperature on Ni-Cu-Fe rod.

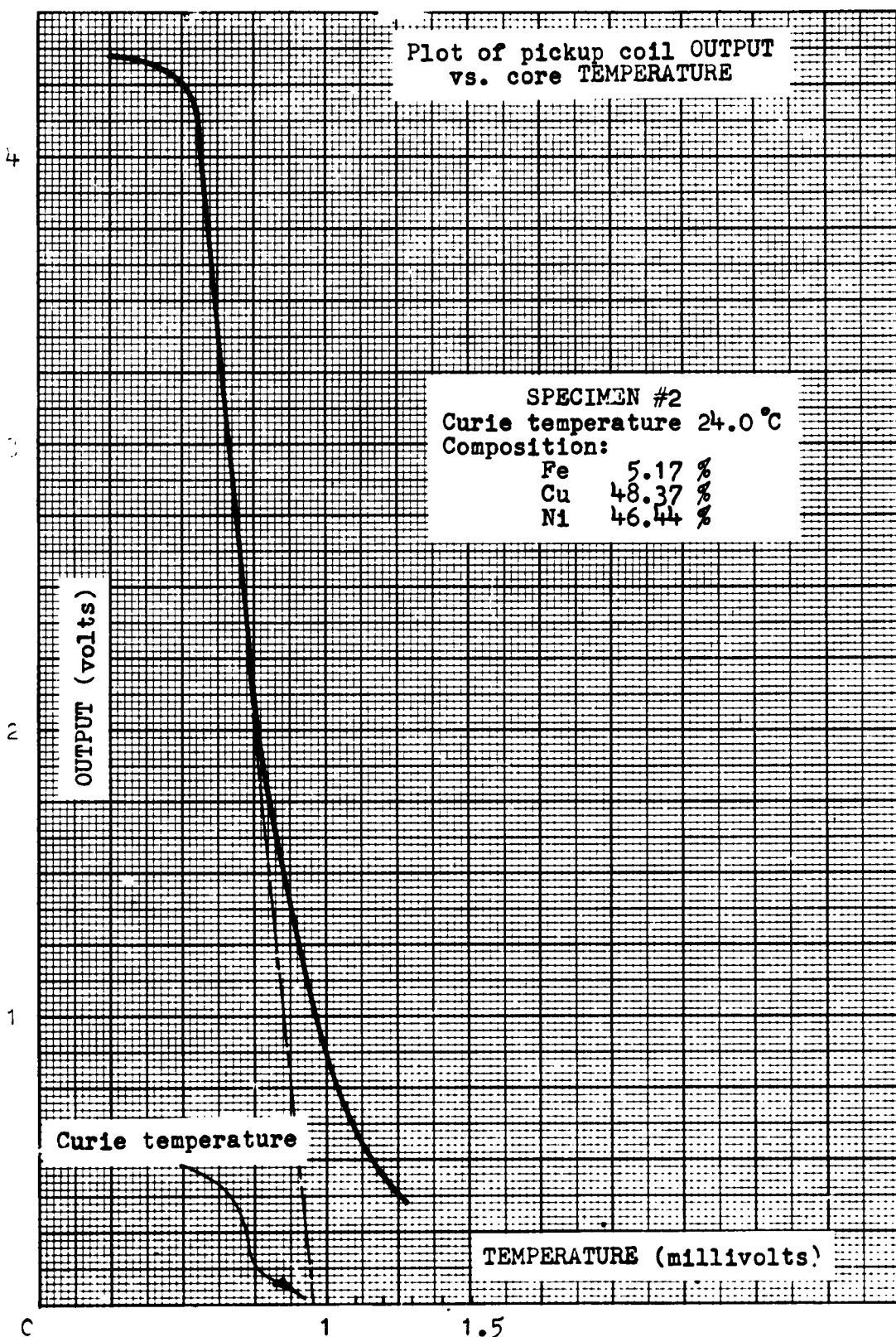


Fig. 19. Measurement of Curie temperature on Ni-Cu-Fe ring.

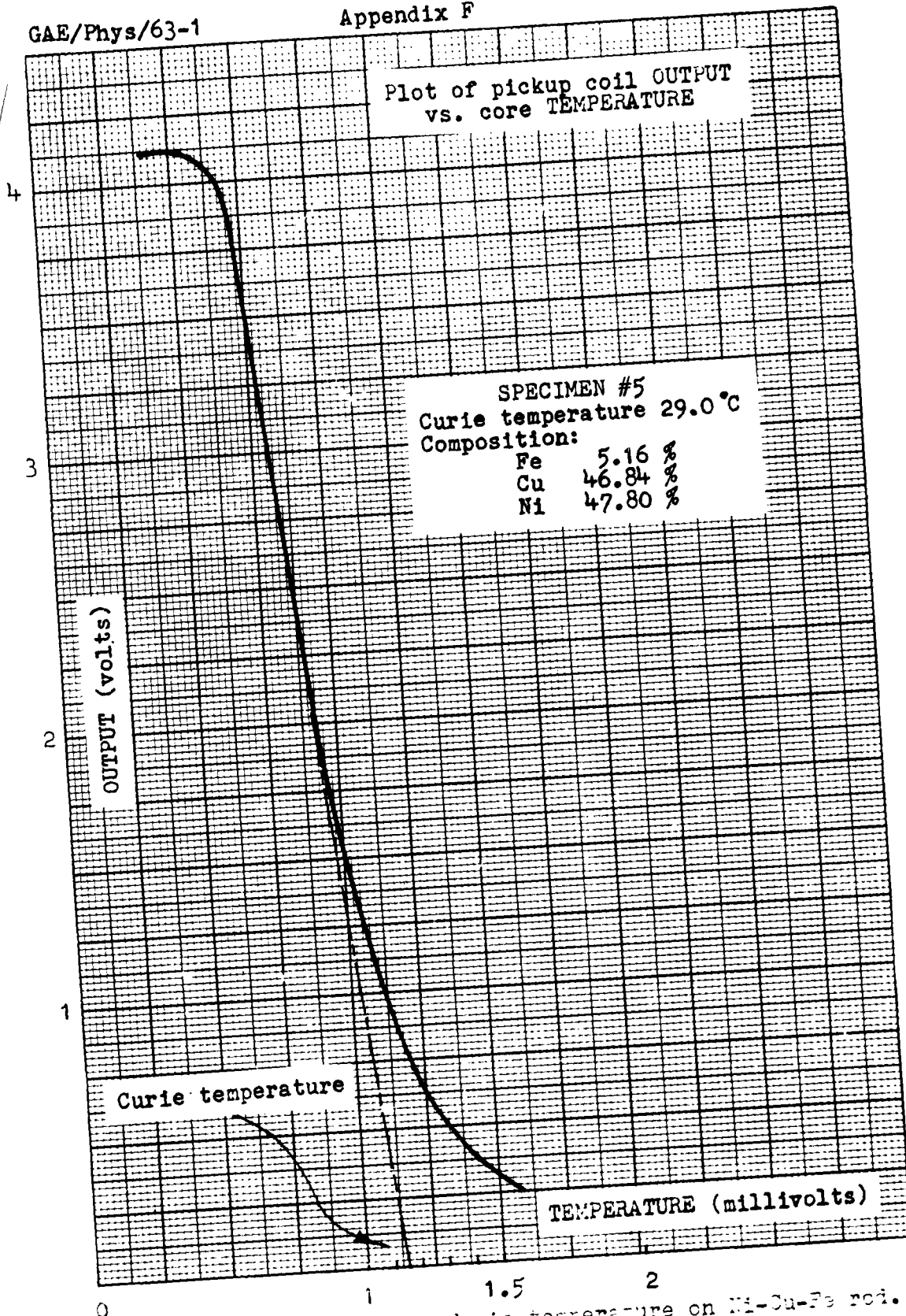


Fig. 20. Measurement of Curie temperature on Ni-Cu-Fe rod.

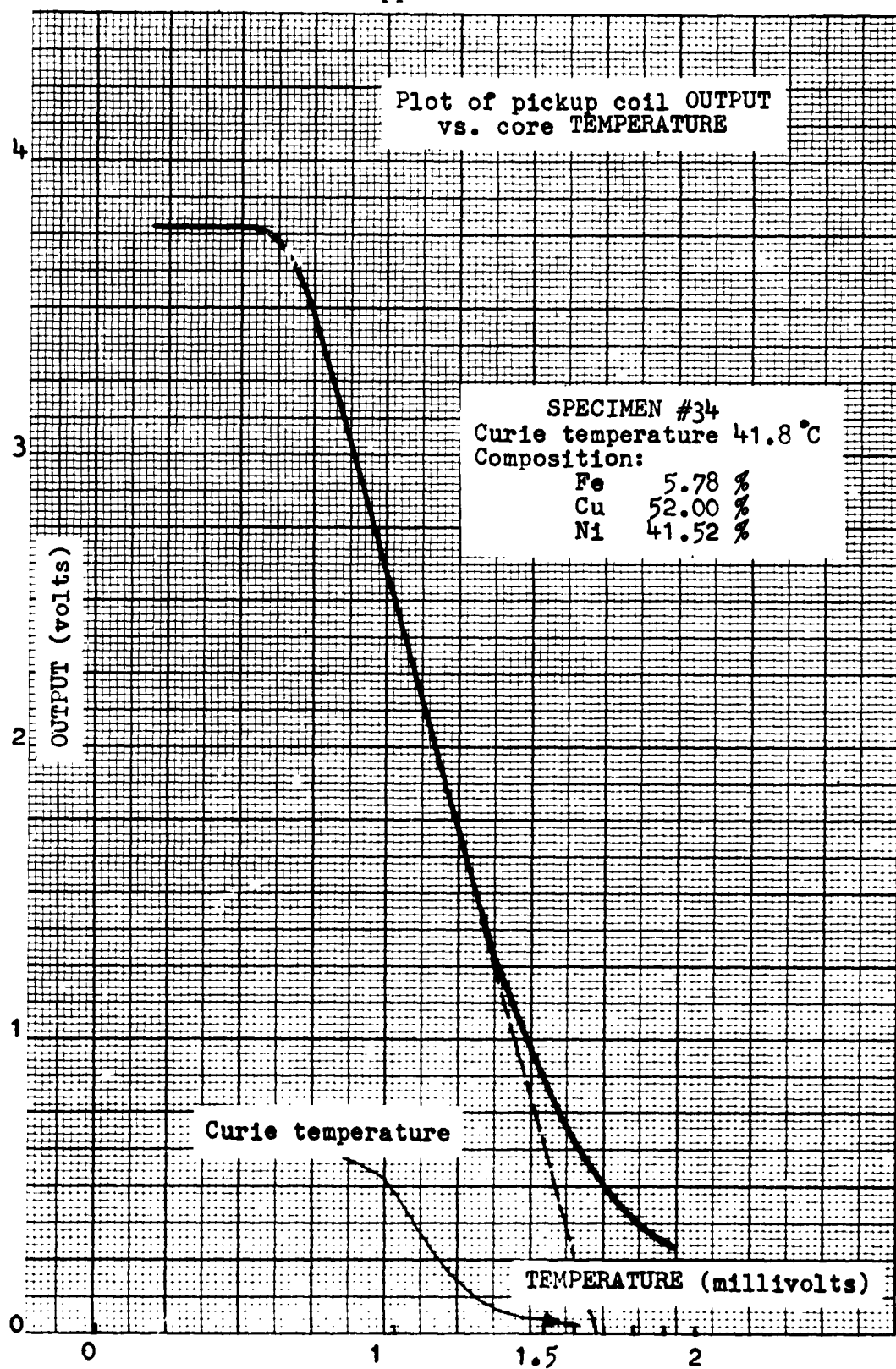


Fig. 21. Measurement of Curie temperature on Ni-Cu-Fe rod.

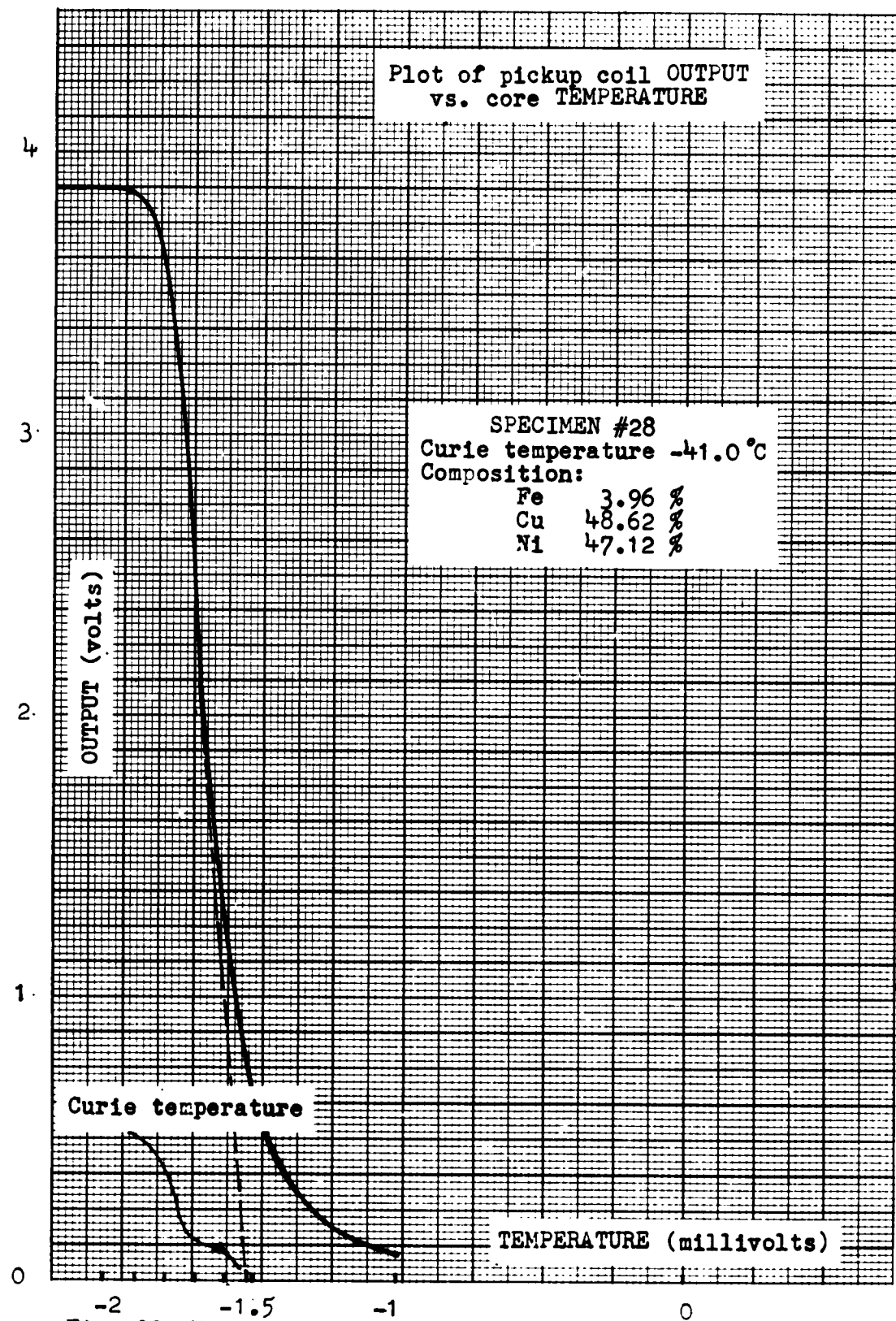


Fig. 22. Measurement of Curie temperature on Ni-Cu-Fe rod.

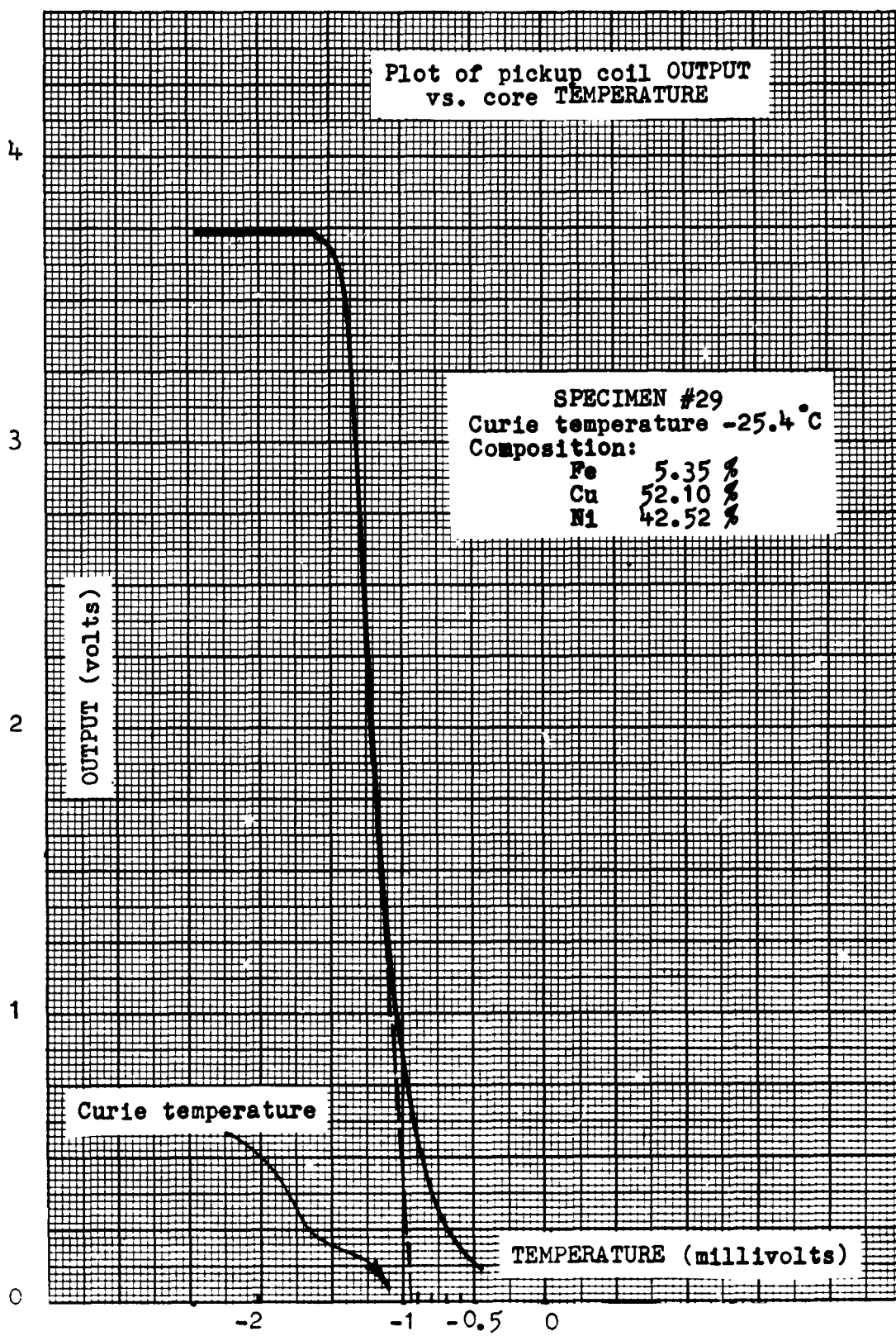


Fig. 23. Measurement of Curie temperature on Ni-Cu-Fe rod.

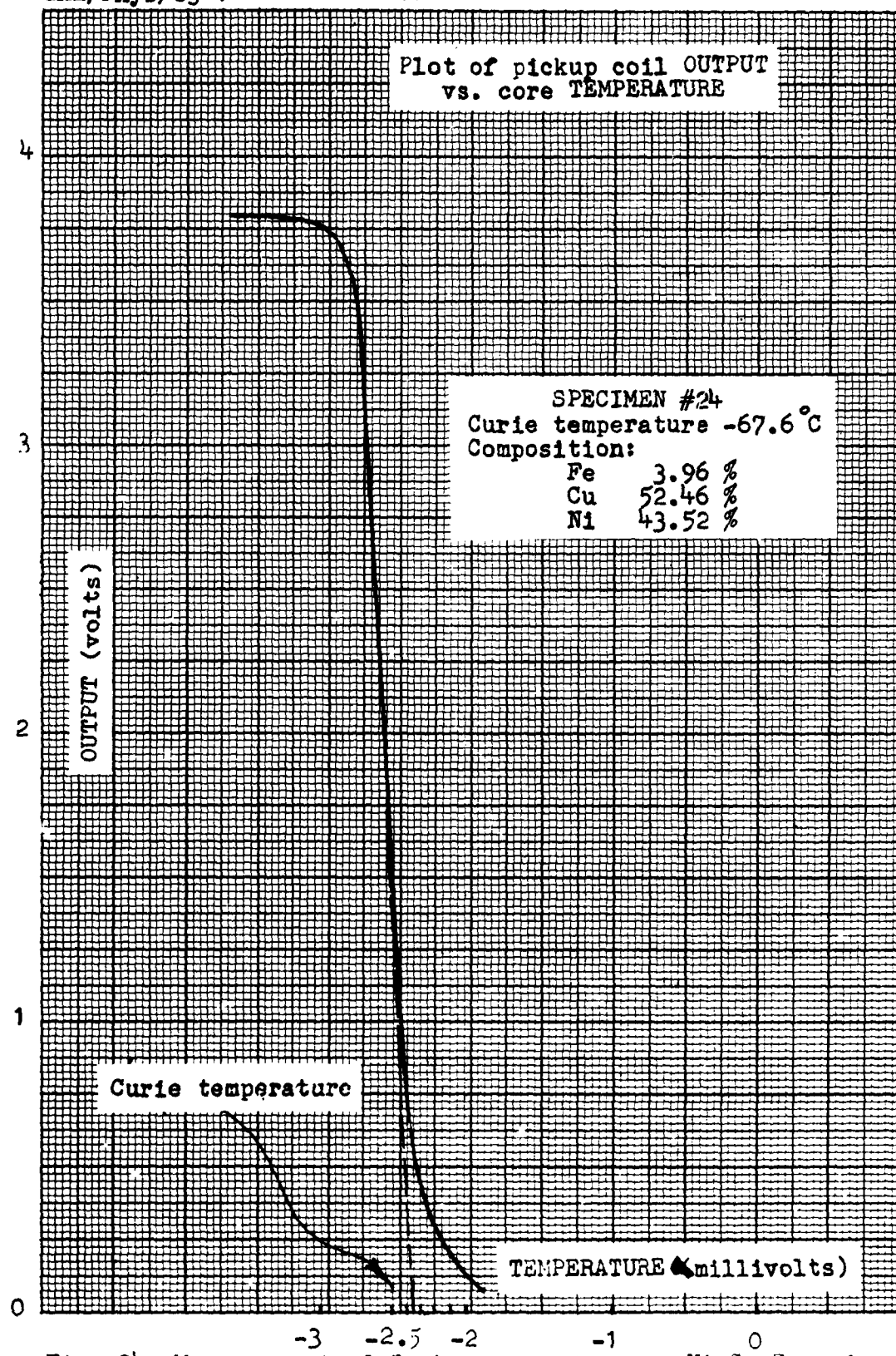


Fig. 24. Measurement of Curie temperature on Ni-Cu-Fe rod.

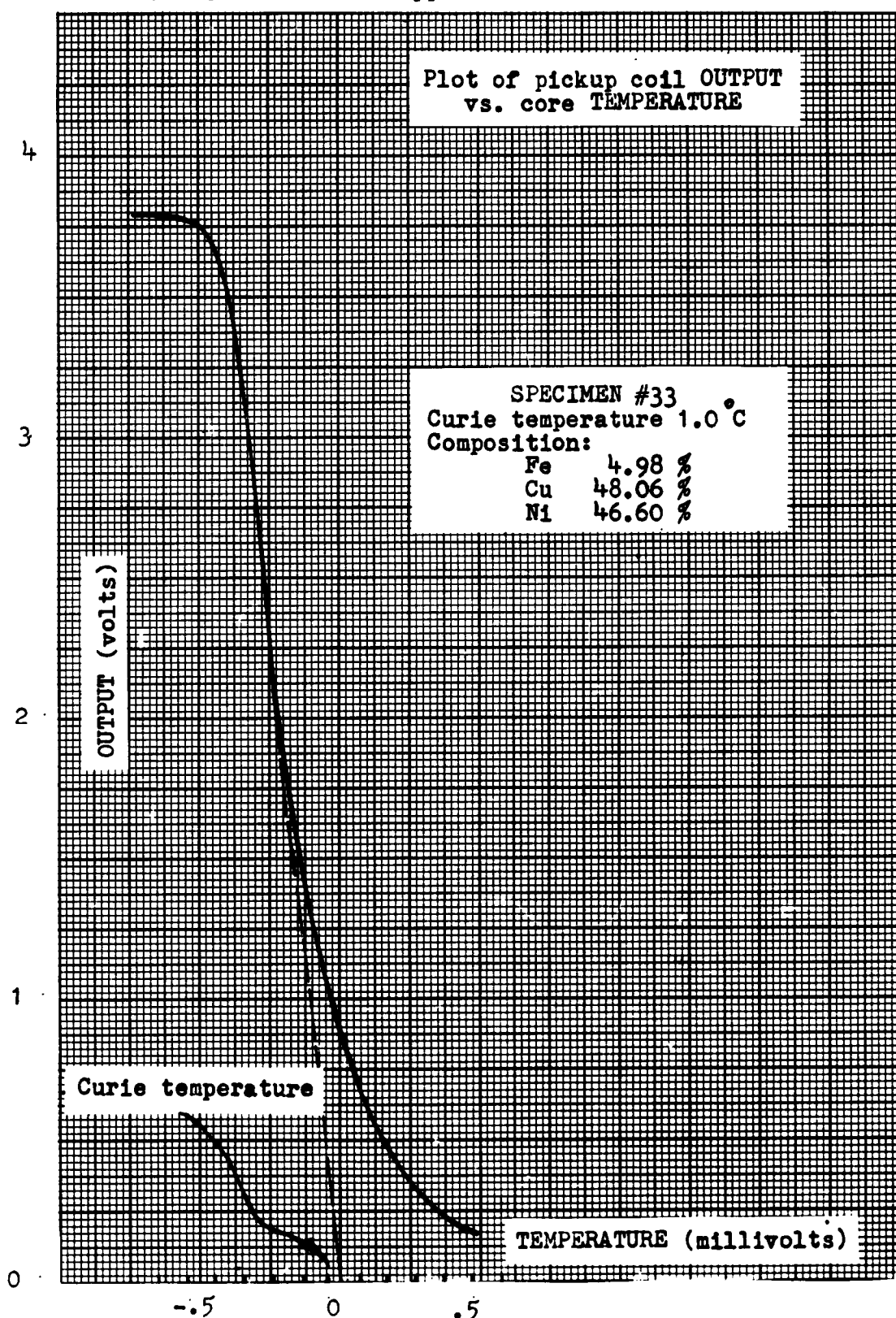


Fig. 25. Measurement of Curie temperature on Ni-Cu-Fe rod.

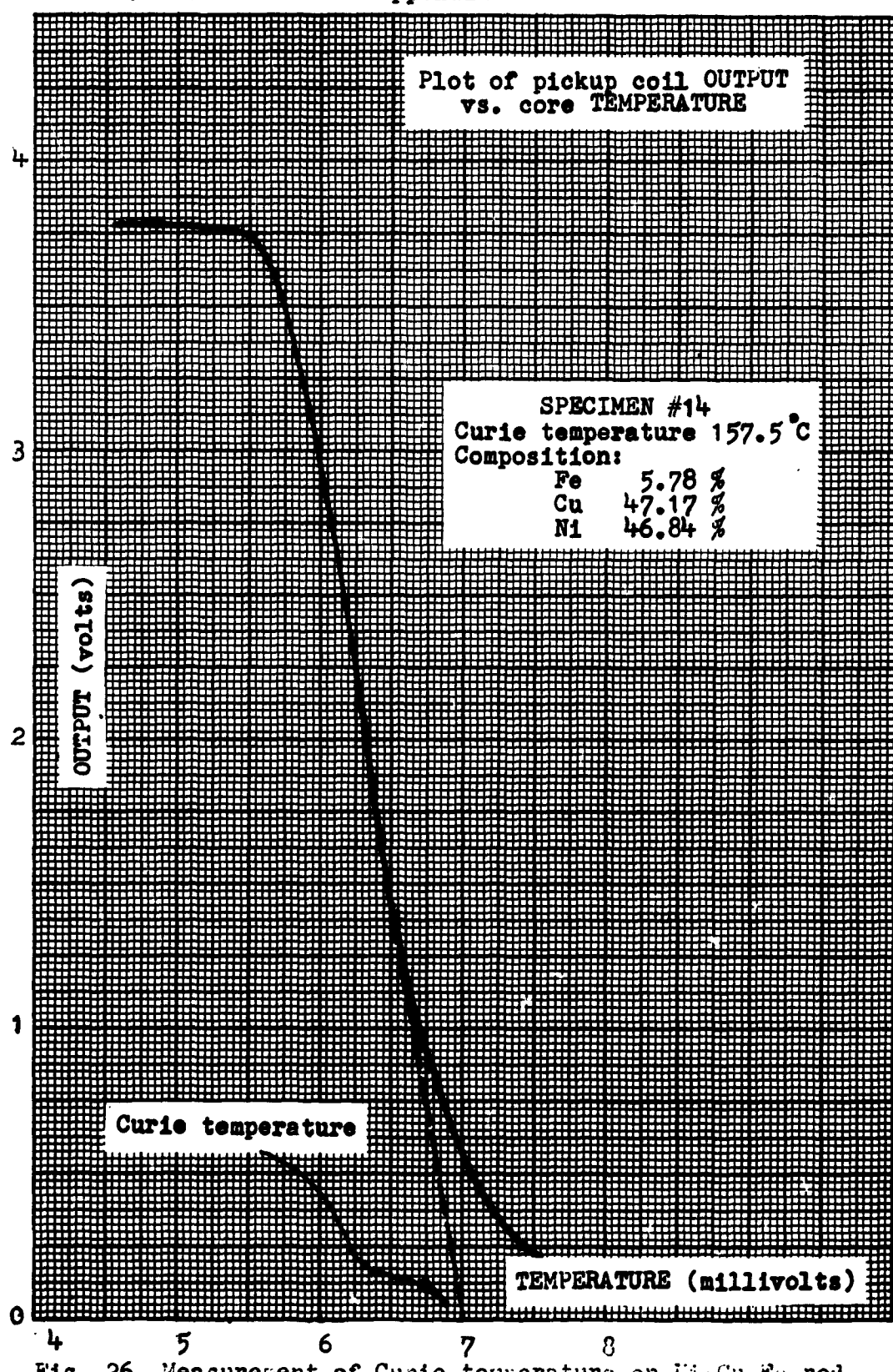


Fig. 26. Measurement of Curie temperature on Ni-Cu-Fe rod.

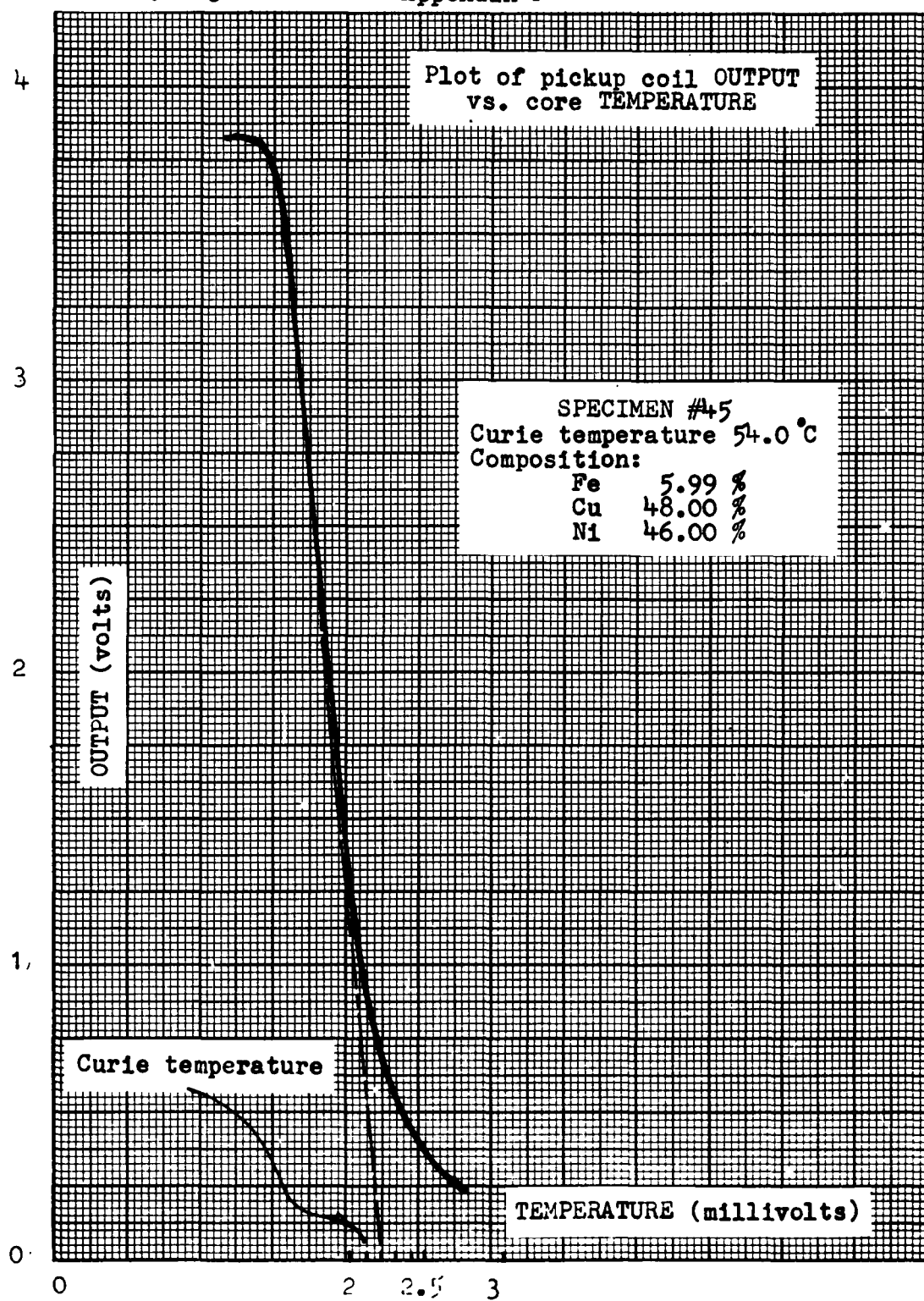


Fig. 27. Measurement of Curie temperature on Ni-Cu-Fe rod.

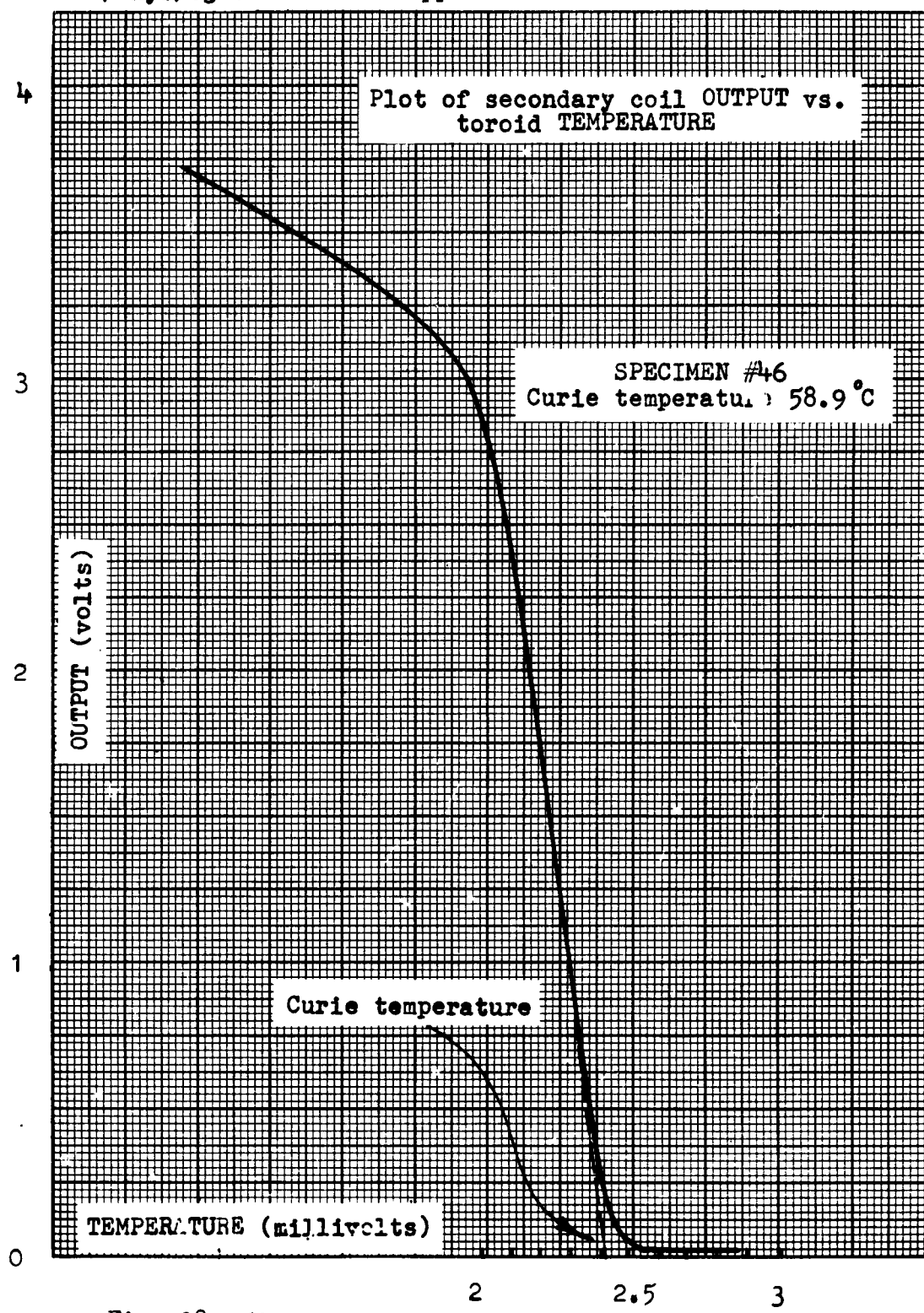


Fig. 28. Measurement of Curie temperature on Ni-Cu-Fe toroid.

SPECIMEN NUMBER	COMPOSITION (%)			CURIE TEMPERATURE °C
	Ni	Cu	Fe	
1	46.36	48.49	5.01	23.0
2	46.44	48.37	5.17	24.0
3	46.80	47.87	4.95	31.2
4	47.36	47.47	5.14	40.8
5	47.80	46.84	5.16	29.0
6	46.12	48.43	5.06	33.5
7	47.40	47.26	5.06	62.5
8	42.40	51.48	6.10	135.6
9	41.20	51.58	6.53	143.6
10	42.24	51.13	6.26	135.0
11	43.56	50.33	5.99	High
12	45.56	48.41	5.99	130.3
13	45.52	47.29	6.96	92.5
14	46.84	47.17	5.78	157.5
15	40.80	51.78	6.96	96.8
15	39.76	52.37	7.17	High

Fig. 29. Experimental results of Curie temperature measurements on Ni-Cu-Fe alloys.

SPECIMEN NUMBER	COMPOSITION (%)			CURIE TEMPERATURE °C
	Ni	Cu	Fe	
17	42.12	50.23	7.38	High
18	42.48	50.50	6.85	High
19	42.76	49.91	6.90	High
20	42.72	49.60	7.01	High
21	48.20	46.64	4.71	Bad Specimen
22	45.88	48.04	5.78	67.5
23	42.88	49.94	6.85	High
24	43.52	52.46	3.96	-67.6
25	44.72	51.06	4.17	-58.3
26	45.68	50.09	4.01	-42.4
27	47.80	51.40	.15	No Fe
28	47.12	48.68	3.96	-41.0
29	42.52	52.10	5.35	-25.4
30	43.68	50.97	4.98	-11.4
31	44.64	50.10	5.19	-10.0
32	45.55	49.08	4.92	-2.4

Fig. 29(continued). Experimental results of Curie temperature measurements on Ni-Cu-Fe alloys.

SPECIMEN NUMBER	COMPOSITION (%)			CURIE TEMPERATURE °C
	Ni	Cu	Fe	
33	46.60	48.06	4.98	1.0
34	41.52	52.00	5.78	41.8
35	42.48	51.03	5.99	36.5
36	44.60	49.05	5.99	55.0
37	45.40	48.01	5.94	53.0
38	45.24	49.65	4.87	-14.6
39	42.64	51.03	6.26	80.8
40	42.60	50.71	6.21	68.0
41	43.80	49.91	6.21	57.5
42	44.24	49.54	5.94	73.4
43	44.48	49.02	5.89	72.0
44	45.24	48.48	5.94	57.5
45	46.00	48.00	5.99	54.0

Fig. 29 (continued). Experimental results of Curie temperature measurements on Ni-Cu-Fe alloys.